50121

(33)

STRATIGRAPHY, PETROGRAPHY, AND MINERALOGY OF BANDELIER TUFF AND CERRO TOLEDO DEPOSITS

by

D. E. Broxton, G.H. Heiken, S. J. Chipera, and F. M. Byers, Jr.

A total of 86 samples was collected in three measured sections on the north wall of Los Alamos Canyon to determine the lithology, petrography, and mineralogy of tuffs at TA 21. Methods of investigation included field observations, modal point counts, petrographic descriptions, x-ray diffraction, and image analysis. These data were collected to develop conceptual models for the hydrogeology of the site, evaluate potential transport pathways and processes, and provide bounds on parameters used in models for evaluating the migration of water and contaminants.

Bedrock stratigraphic units in Los Alamos Canyon consists of (in ascending order) the Otowi Member of the Bandelier Tuff, epiclastic deposits of the Cerro Toledo interval, and the Tshirege Member (including the Tsankawi Pumice Bed) of the Bandelier Tuff. The exposed upper 18 to 21 m of the Otowi Member is a simple cooling unit made up of massive, nonwelded, vitric ignimbrite. The Otowi Member is easily eroded and crops out as gentle slopes near the bottom of Los Alamos Canyon. The Cerro Toledo interval is an informal name given to a complex sequence of epiclastic sediments and tephras of mixed provenance. This unit contains deposits normally assigned to the Cerro Toledo Rhyolite, including well-stratified tuffaceous sandstones and siltstones as well as primary ash-fall and pumice-fall deposits. The Cerro Toledo interval also contains intercalated deposits not normally assigned to the Cerro Toledo Rhyolite; these include sand, gravel, cobble, and boulder deposits derived from the Tschicoma Formation. The thickness of the Cerro Toledo interval ranges from 3 to 9 m. The Tsankawi Pumice Bed is a 0.7- to 0.9-m-thick rhyolitic pumice-fall deposit that consists of two normally graded pumice falls separated by a thin ash bed. The Tshirege Member is a multiple-flow rhyolitic ignimbrite that forms a series of step-like vertical cliffs and sloping ledges in Los Alamos Canyon. It is a compound cooling unit whose physical properties vary both vertically and laterally; the thickness of this unit ranges from 89 to 98 m.

Received by ER-RPF
OCT 30 1995
Dic

10443

The bulk-rock mineralogy of tuffs at TA-21 consists primarily of alkali feldspar + quartz ± cristobalite ± tridymite ± glass. Minor constituents include smectite, hornblende, mica, hematite, calcite, and kaolinite. Volcanic glass is the dominant constituent in the Otowi Member, tuffs of the Cerro Toledo interval, and the lower part of the Tshirege Member. The upper two-thirds of the Tshirege Member have undergone extensive devitrification and vapor-phase alteration; the mineral assemblage in these tuffs consists of alkali feldspar + quartz ± cristobalite ± tridymite. Smectite and hematite occur in small (<2%) amounts throughout the stratigraphic sequence. These two trace minerals are important because they are highly sorptive of certain radionuclides and could provide important natural barriers to their migration. Although these minerals occur in small quantities, they are disseminated throughout all stratigraphic units, and their aggregate abundance and surface area are large when integrated over long groundwater flow paths through the tuffs.

The exposed tuffaceous rocks at TA-21 are provisionally subdivided into eight hydrogeological units based upon their lithological and mineralogical properties. Complete delineation of all hydrogeological units at TA-21 must await characterization of subsurface units and systematic measurements of hydrological properties from all rock units.

INTRODUCTION

This study is conducted as part of on-going ER Program RFI work for OU 1106 located at TA-21 (Fig. 1). This report supports the RFI studies by providing geological data for developing and testing hydrogeological conceptual models for the site, evaluating potential transport pathways and processes, and collecting data for parameters used in models for evaluating the migration of water and contaminants. The data also provide a geological framework for evaluating various types of remediation that could be applied at the site. This study supports these goals by delineating important hydrogeological units whose physical and chemical properties control the movement of moisture and contaminants.

The general stratigraphy of tuffaceous rocks of the Pajarito Plateau is described by Bailey *et al.* (1969), Baltz *et al.* (1963), Weir and Purtymun (1962), Griggs (1964), Smith *et al.* (1970), Crowe *et al.* (1978), Heiken *et al.* (1986), Vaniman and Wohletz (1990 and 1991), and Gardner *et al.* (1993). This report builds on the earlier studies and provides geological information specific to TA-21. It includes information about vertical and lateral changes in lithology, petrography, and mineralogy within the tuffs that underlie the SWMUs at TA-21. Together, the geologic map (Goff, Sec. II, this report) and this paper provide a stratigraphic framework for future studies.

Reneau (Sec. V, this report) describes geomorphic characteristics of TA-21, as well as post-Bandelier deposits not discussed here. This paper documents some observations about fracture characteristics at TA-21, but the data presented may have only local significance and should be used as supplemental information to the more systematic study of fractures by Wohletz (Sec. III, this report). An ongoing study of fracture mineralogy by D. Vaniman, LANL, is evaluating the potential for contaminant transport within fractures

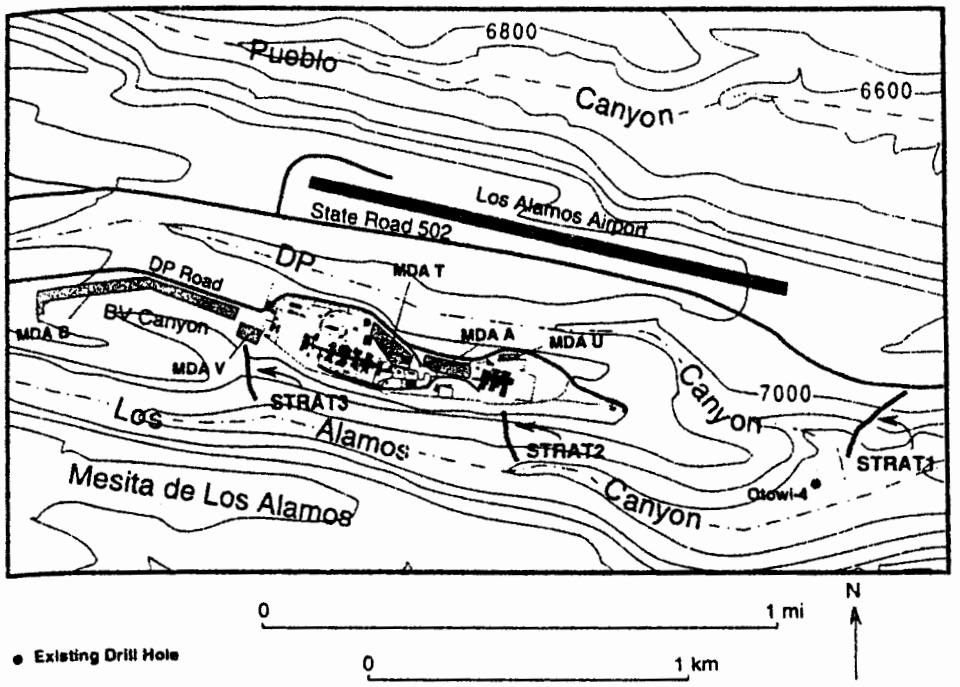

Fig. 1. Map showing the locations of the three stratigraphic sections (for example, STRAT-1) measured on the north wall of Los Alamos Canyon at TA-21.

by examining these structures for evidence of past groundwater transport. Vaniman's study also is identifying mineral assemblages that may retard contaminant transport in fractures.

METHODS

For this study, 86 bulk-rock samples were collected from outcrops of bedrock units exposed on the north wall of Los Alamos Canyon. Three stratigraphic sections were measured and sampled (Fig. 1). Section OU-1106-STRAT-1 (34 samples), near the confluence of DP Canyon and Los Alamos Canyon, is the easternmost of the three sections. Section OU-1106-STRAT-2 (25 samples) is south of MDA U in the eastern part of the TA-21 complex. Section OU-1106-STRAT-3 (27 samples), south of MDA V, is the westernmost section. Samples were collected at a nominal vertical spacing of 5 m or at major changes in lithology. Metal tags mark sample sites in the field. Initially, vertical control was maintained by Jacob staff and Abney level. Later, Merrick & Company surveyed locations and elevations of all sample sites (Table I).

Field work was performed under procedures described in LANL-ER-SOP-03.07 (*Characterization of Lithologic Variations within the Rock Outcrops of a Volcanic Field*). Observations at each sample site generally include descriptions of rock type, type and degree of alteration, welding and compaction, phenocryst assemblage and abundance, color on fresh and weathered surfaces, pumice size and abundance, and weathering characteristics. Bedding characteristics, fractures and their filling materials, and lithic assemblage, size, and abundance were also noted.

TABLE I

Location of Samples Collected in Stratigraphic Sections at TA-21

Sample Number	Stratigraphic Unit [a]	Location Identification	Bar Code Number	Coordinates North (ft) [b]	Coordinates East (ft) [b]	Latitude [c]	Longitude [c]	Elevation (ft)
Stratigraphic Section #1 (Easternmost Section)								
OU-1106-STRAT1-1	Qbo	21-1485	AAA2549	1637857	1773468	35 52 28.16223	106 15 23.98251	6662.9
OU-1106-STRAT1-2	Qbo	21-1486	AAA2550	1637736	1773513	35 52 28.24855	106 15 22.88122	6683.4
OU-1106-STRAT1-3	Qbo	21-1487	AAA2551	1637730	1773554	35 52 28.65329	106 15 22.74758	6692.7
OU-1106-STRAT1-4	Qbo	21-1488	AAA2552	1637793	1773556	35 52 28.42660	106 15 22.02381	6715.8
OU-1106-STRAT1-5	Qbo	21-1489	AAA2553	1637767	1773585	35 52 28.77987	106 15 22.17646	6726.1
OU-1106-STRAT1-6	Qct	21-1490	AAA2554	1637802	1773582	35 52 28.61254	106 15 21.81482	6722.0
OU-1106-STRAT1-7	Qct	21-1491	AAA2555	1637801	1773582	35 52 28.61228	106 15 21.82369	6722.3
OU-1106-STRAT1-8	Qct	21-1492	AAA2556	1637803	1773582	35 52 28.61068	106 15 21.79562	6723.7
OU-1106-STRAT1-9	Qct	21-1493	AAA2557	1637803	1773582	35 52 28.60573	106 15 21.79343	6726.4
OU-1106-STRAT1-10	Qct	21-1494	AAA2558	1637805	1773583	35 52 28.60683	106 15 21.78694	6727.5
OU-1106-STRAT1-11	Qbt-1g	21-1495	AAA2559	1637831	1773577	35 52 28.44729	106 15 21.51588	6727.3
OU-1106-STRAT1-12	Qbt-1g	21-1496	AAA2560	1637833	1773577	35 52 28.44223	106 15 21.49522	6729.2
OU-1106-STRAT1-13	Qbt-1g	21-1497	AAA2561	1637833	1773577	35 52 28.44209	106 15 21.49060	6729.5
OU-1106-STRAT1-14	Qbt-1g	21-1498	AAA2562	1637826	1773577	35 52 28.46674	106 15 21.56521	6731.3
OU-1106-STRAT1-15	Qbt-1g	21-1499	AAA2563	1637828	1773577	35 52 28.46022	106 15 21.54563	6732.3
OU-1106-STRAT1-16	Qbt-1g	21-1500	AAA2564	1637856	1773583	35 52 28.41357	106 15 21.21451	6747.4
OU-1106-STRAT1-17	Qbt-1g	21-1501	AAA2565	1637878	1773578	35 52 28.27199	106 15 20.98241	6763.2
OU-1106-STRAT1-18	Qbt-1g	21-1502	AAA2566	1637907	1773582	35 52 28.19501	106 15 20.64471	6779.2
OU-1106-STRAT1-19	Qbt-1g	21-1503	AAA2567	1637936	1773577	35 52 28.03657	106 15 20.35014	6794.9
OU-1106-STRAT1-20	Qbt-1g	21-1504	AAA2568	1637932	1773595	35 52 28.21381	106 15 20.29730	6810.4
OU-1106-STRAT1-21	Qbt-1v	21-1505	AAA2569	1637972	1773613	35 52 28.22467	106 15 19.77126	6827.1
OU-1106-STRAT1-22	Qbt-1v	21-1506	AAA2570	1638063	1773630	35 52 28.01135	106 15 18.67055	6843.3
OU-1106-STRAT1-23	Qbt-1v	21-1507	AAA2571	1638099	1773640	35 52 27.89166	106 15 18.23306	6856.8
OU-1106-STRAT1-24	Qbt-1v	21-1508	AAA2572	1638133	1773653	35 52 27.88309	106 15 17.79429	6875.5
OU-1106-STRAT1-25	Qbt-1v	21-1509	AAA2573	1638164	1773668	35 52 27.94536	106 15 17.38887	6891.5
OU-1106-STRAT1-26	Qbt-1v	21-1510	AAA2574	1638201	1773682	35 52 27.92736	106 15 16.88596	6908.5
OU-1106-STRAT1-27	Qbt-2	21-1511	AAA2575	1638221	1773703	35 52 28.03250	106 15 16.55617	6924.1
OU-1106-STRAT1-28	Qbt-2	21-1512	AAA2576	1638255	1773722	35 52 28.07319	106 15 16.08919	6941.3
OU-1106-STRAT1-29	Qbt-2	21-1513	AAA2577	1638287	1773743	35 52 28.13243	106 15 15.63606	6957.5
OU-1106-STRAT1-30	Qbt-nw	21-1514	AAA2578	1638313	1773764	35 52 28.40968	106 15 15.16071	6974.2
OU-1106-STRAT1-31	Qbt-3	21-1515	AAA2579	1638340	1773790	35 52 28.34285	106 15 14.80976	6990.1
OU-1106-STRAT1-32	Qbt-3	21-1516	AAA2580	1638367	1773812	35 52 28.44040	106 15 14.40026	7006.4
OU-1106-STRAT1-33	Qbt-3	21-1517	AAA2581	1638394	1773833	35 52 28.52247	106 15 13.99805	7023.4
OU-1106-STRAT1-34	Qbt-3	21-1518	AAA2582	1638414	1773850	35 52 28.59649	106 15 13.68466	7036.2
Stratigraphic Section #2 (Central DP Mesa)								
OU-1106-STRAT2-1	Qbo	21-1519	AAA2583	1634069	1773288	35 52 25.19541	106 16 15.04309	6746.4
OU-1106-STRAT2-2	Qbo	21-1520	AAA2584	1634060	1773315	35 52 25.45641	106 16 15.14924	6761.3
OU-1106-STRAT2-3	Qct	21-1521	AAA2585	1634061	1773331	35 52 25.61154	106 16 15.13543	6769.7
OU-1106-STRAT2-4	Qct	21-1522	AAA2586	1634062	1773332	35 52 25.62654	106 16 15.12766	6771.2
OU-1106-STRAT2-5	Qbt-1g	21-1523	AAA2587	1634046	1773357	35 52 25.87707	106 16 15.31583	6788.0
OU-1106-STRAT2-6	Qbt-1g	21-1524	AAA2588	1634037	1773377	35 52 26.06879	106 16 15.42439	6800.9
OU-1106-STRAT2-7	Qbt-1g	21-1525	AAA2589	1634032	1773401	35 52 26.30941	106 16 15.48825	6818.6
OU-1106-STRAT2-8	Qbt-1g	21-1526	AAA2590	1634019	1773424	35 52 26.54063	106 16 15.65041	6831.8
OU-1106-STRAT2-9	Qbt-1g	21-1527	AAA2591	1634004	1773449	35 52 26.78304	106 16 15.82704	6847.4
OU-1106-STRAT2-10	Qbt-1g	21-1528	AAA2592	1633991	1773462	35 52 26.91627	106 16 15.99124	6858.1
OU-1106-STRAT2-11	Qbt-1g	21-1529	AAA2593	1633961	1773470	35 52 26.99011	106 16 16.35070	6873.5
OU-1106-STRAT2-12	Qbt-1g	21-1530	AAA2594	1633961	1773479	35 52 27.08237	106 16 16.35146	6886.5
OU-1106-STRAT2-13	Qbt-1g	21-1531	AAA2595	1633970	1773486	35 52 27.14746	106 16 16.24466	6889.0
OU-1106-STRAT2-14	Qbt-1v	21-1532	AAA2596	1633973	1773548	35 52 27.78515	106 16 16.20145	6906.6
OU-1106-STRAT2-15	Qbt-1v	21-1533	AAA2597	1633970	1773574	35 52 28.02387	106 16 16.24818	6923.7
OU-1106-STRAT2-16	Qbt-1v	21-1534	AAA2598	1633976	1773579	35 52 28.08672	106 16 16.16677	6941.2
OU-1106-STRAT2-17	Qbt-2	21-1535	AAA2599	1633996	1773593	35 52 28.20469	106 16 15.90615	6958.2
OU-1106-STRAT2-18	Qbt-2	21-1536	AAA2600	1634053	1773609	35 52 28.37063	106 16 15.23458	6977.1
OU-1106-STRAT2-19	Qbt-2	21-1537	AAA2601	1634031	1773618	35 52 28.45657	106 16 15.50194	6998.0
OU-1106-STRAT2-20	Qbt-2	21-1538	AAA2602	1634023	1773635	35 52 28.62002	106 16 15.59348	7015.8
OU-1106-STRAT2-21	Qbt-nw	21-1539	AAA2603	1634028	1773669	35 52 28.96302	106 16 15.53294	7025.9
OU-1106-STRAT2-22	Qbt-3	21-1540	AAA2604	1634054	1773699	35 52 29.25793	106 16 15.22048	7053.8
OU-1106-STRAT2-23	Qbt-3	21-1541	AAA2605	1634054	1773711	35 52 29.37201	106 16 15.22184	7069.3
OU-1106-STRAT2-24	Qbt-3	21-1542	AAA2606	1634060	1773745	35 52 29.71054	106 16 15.14859	7086.7
OU-1106-STRAT2-25	Qbt-3	21-1570	AAA5678	1634076	1773738	35 52 29.63926	106 16 14.95713	7103.0

[a] *Stratigraphic Unit - Nomenclature of Vaniman and Wohletz (1990, 1991); Qbo = Otowi Member of the Bandelier Tuff; Qct = Cerro Toledo interval; Qbt-1g = Tshirege unit 1g; Qbt-1v = Tshirege unit 1v; Qbt-2 = Tshirege unit 2; Qbt-nw = nonwelded tuff; Qbt-3 = Tshirege unit 3.*

[b] *State plane coordinate system NAD 83.*

[c] *Degrees, minutes, and seconds.*

TABLE I (cont)

LOCATION OF SAMPLES COLLECTED IN STRATIGRAPHIC SECTIONS AT TA-21

Sample Number	Stratigraphic Unit[a]	Location Identification	Bar Code Number	Coordinates North (ft)[b]	Coordinates East (ft)[b]	Latitude[c]			Longitude[c]			Elevation (ft)
Stratigraphic Section #3 (Westernmost Section)												
OU 1106-STRAT3-1	Qbo	21-1543	AAA2607	1631540	1773813	35	52	30.37632	106	16	45.77789	6779.1
OU 1106-STRAT3-2	Qct	21-1544	AAA2608	1631480	1774005	35	52	32.27278	106	16	46.50356	6831.9
OU 1106-STRAT3-3	Qct	21-1545	AAA2609	1631475	1774032	35	52	32.54528	106	16	46.55871	6849.5
OU 1106-STRAT3-4	Qct	21-1546	AAA2610	1631475	1774032	35	52	32.54385	106	16	46.56527	6850.[illegible]
OU 1106-STRAT3-5	Qct	21-1547	AAA2611	1631464	1774034	35	52	32.53960	106	16	46.69725	6851.3
OU 1106-STRAT3-6	Qct	21-1548	AAA2612	1631457	1774037	35	52	32.59136	106	16	46.78694	6861.4
OU 1106-STRAT3-7	Qbt 1g	21-1549	AAA2613	1631445	1774036	35	52	32.58614	106	16	46.92624	6864.7
OU 1106-STRAT3-8	Qbt 1g	21-1550	AAA2614	1631442	1774043	35	52	32.64717	106	16	46.96656	6867.[illegible]
OU 1106-STRAT3-9	Qbt 1g	21-1551	AAA2615	1631419	1774061	35	52	32.83190	106	16	47.23737	6885.5
OU 1106-STRAT3-10	Qbt 1g	21-1552	AAA2616	1631409	1774077	35	52	32.9[illegible]52	106	16	47.38636	6901.5
OU 1106-STRAT3-11	Qbt 1g	21-1553	AAA2617	1631401	1774101	35	52	33.22538	106	16	47.45172	69[illegible]
OU 1106-STRAT3-12	Qbt 1g	21-1554	AAA2618	1631392	1774118	35	52	33.39489	106	16	47.57456	6931.[illegible]
OU 1106-STRAT3-13	Qbt 1g	21-1555	AAA2619	1631392	1774121	35	52	33.42131	106	16	47.56606	6933.2
OU 1106-STRAT3-14	Qbt 1v	21-1556	AAA2620	1631395	1774119	35	52	33.40229	106	16	47.53020	6934.3
OU 1106-STRAT3-15	Qbt 1v	21-1557	AAA2621	1631393	1774121	35	52	33.42113	106	16	47.56266	6937.9
OU 1106-STRAT3-16	Qbt 1v	21-1558	AAA2622	1631373	1774139	35	52	33.60113	106	16	47.79883	6954.3
OU 1106-STRAT3-17	Qbt 1v	21-1559	AAA2623	1631363	1774158	35	52	33.78689	106	16	47.92711	6968.6
OU 1106-STRAT3-18	Qbt 1v	21-1560	AAA2624	1631373	1774175	35	52	33.95934	106	16	47.80735	6985.6
OU 1106-STRAT3-19	Qbt 2	21-1561	AAA2625	1631300	1774213	35	52	34.33600	106	16	48.68449	6999.0
OU 1106-STRAT3-20	Qbt 2	21-1562	AAA2626	1631292	1774220	35	52	34.39941	106	16	48.78404	7014.6
OU 1106-STRAT3-21	Qbt 2	21-1563	AAA2627	1631168	1774217	35	52	34.37489	106	16	50.29901	7048.[illegible]
OU 1106-STRAT3-22	Qbt nw	21-1564	AAA2628	1631199	1774288	35	52	35.07360	106	16	49.91321	7063.[illegible]
OU 1106-STRAT3-23	Qbt nw	21-1565	AAA2629	1631271	1774351	35	52	35.69898	106	16	49.03948	7084.[illegible]
OU 1106-STRAT3-24	Qbt 3	21-1566	AAA2630	1631301	1774372	35	52	35.90971	106	16	48.68351	7100.6
OU 1106-STRAT3-25	Qbt 3	21-1567	AAA2631	1631306	1774395	35	52	36.13487	106	16	48.61992	7117.[illegible]
OU 1106-STRAT3-26	Qbt 3	21-1568	AAA2632	1631319	1774416	35	52	36.33778	106	16	48.48275	713[illegible]
OU 1106-STRAT3-27	Qbt 3	21-1569	AAA2633	1631316	1774453	35	52	36.90362	106	16	48.49517	7150.8

The mineralogy of all 86 bulk-rock samples was characterized by x-ray diffraction analyses (XRD). Samples were first powdered in a tungsten-carbide shatter box and then mixed with an internal standard of 1-µm metallurgical-grade Al_2O_3 (corundum) powder in a ratio of 80% sample to 20% internal standard by weight. The samples were then ground under acetone in an automatic Brinkmann-Retsch mill fitted with an agate mortar and pestle to produce an average particle size of <5 µm. This fine size is necessary to ensure adequate particle statistics and to minimize primary extinction (Klug and Alexander 1974, pp. 365-367). Particle-size distributions have been verified using a Horiba CAPA-500 centrifugal particle-size distribution analyzer calibrated with Duke Scientific glass microsphere standards.

The XRD data were collected on a Siemens D-500 theta-theta diffractometer using copper-Kα radiation, incident- and diffracted-beam Soller slits, and a Kevex solid-state (SiLi) detector. Data were typically collected from 2.0 to 50.0° 2θ using a 0.02° step size and at least 2 s per step. Quantitative analyses employed the internal standard or "matrix-flushing" method of Chung (1974a,b), which requires adding an internal standard to each sample. Details for analysis can be found in Bish and Chipera (1988; 1989). In addition, the following YMP procedures were used for sample preparation and analysis of XRD samples: LANL-EES-DP-130 (*Geologic Sample Preparation*), LANL-EES-DP-56 (*Brinkmann Automated Grinder Procedure*), LANL-EES-DP-16 (*Siemens X-Ray Diffraction Procedure*), and LANL-EES-DP-116

(*Quantitative X-Ray Diffraction Data Reduction Procedure*). The YMP quality assurance requirements are comparable in rigor to those used by the Los Alamos ER Program.

Thin-section modal point counts were made on 23 of the 25 bulk rock samples and on one pumice lump from section OU-1106-STRAT2 (bulk rock sample #8 was not prepared in time for analysis). Between 2374 and 6057 gridded points were counted for each thin section. The point counts tallied percentages of phenocrysts, lithic fragments, pumice, shards, perlite chips (solid glass or altered glass fragments), and voids, following the draft procedure LANL-ER-SOP-03.05 (*Determination of Volume Constituents in Thin Sections of Rock*). Thin sections were prepared according to YMP procedure LANL-EES-DP-130 (*Geologic Sample Preparation*). Opaque oxide minerals were qualitatively identified using criteria outlined in YMP procedure TWS-ESS-DP-128 (*Procedure for Counting Opaque Minerals in Polished Thin Sections*). Image analysis with a microscope (200x, reflected light) attached to a mini-computer was used to determine magnetite abundances as well as statistics for grain areas, grain dimensions, and grain perimeters for two samples (OU-1106-STRAT2-16 and OU-1106-STRAT3-10). Additional petrographic observations of textures, alteration features, and accessory minerals were collected using procedure LANL-ER-SOP-03.04 (*Petrography*).

RESULTS AND DISCUSSION

Plate 1 in the pocket of this volume is the geologic map of TA-21 by Goff (Sec. II, this report) and Reneau (Sec. V, this report). Plate 2 contains detailed lithologic logs for the three stratigraphic sections measured in this study. Table I correlates sample field numbers with site identifiers and lists the surveyed coordinates of samples. Table II and Fig. 2 present modal petrographic data for stratigraphic section OU-1106-STRAT2; Fig. 3 correlates stratigraphic nomenclature used in this report (that of Vaniman and Wohletz (1990, 1991) with the nomenclature used by earlier workers. Table III and Fig. 4 summarize the field data for the vapor-phase notch, an important stratigraphic marker horizon in the Tshirege Member of the Bandelier Tuff. Table IV and Fig. 5 summarize mineralogical data for all three stratigraphic sections.

Lithologic Characteristics of Tuffs in Los Alamos Canyon

The stratigraphic sequence is similar in each of the three measured sections and consists of (in ascending order) the Otowi Member of the Bandelier Tuff (1.613 ± 0.011 Ma; Izett and Obradovich, 1994), epiclastic sediments and tephras of the Cerro Toledo interval, and the Tshirege Member of the Bandelier Tuff (1.223 ± 0.018 Ma; Izett and Obradovich, 1994). Within the Tshirege Member, mappable subunits are described separately because of their distinct physical properties. Reneau (Sec. V, this report) describes younger soils and alluvial deposits for TA-21.

In this report, we use the term *ignimbrite* to describe all deposits formed by the emplacement of pyroclastic flows. The term *surge beds* is used to describe laminated ash deposits with sandwaves and to refer to pyroclastic surge deposits of any type, including ground-surge, ash-cloud, and base-surge deposits (Fisher and Schmincke, 1984). A *simple cooling unit* is made up of a single pyroclastic flow or successive pyroclastic flows that were emplaced at essentially uniform temperature and cooled as a unit without a break in time or cooling properties (Smith, 1960a,b). A *compound cooling unit* is made up of successive pyroclastic flows emplaced at radically different temperatures and/or emplaced over a sufficiently long period of time that abrupt changes in the temperature gradient caused welding and crystallization patterns to deviate from those found in a simple cooling unit (Smith, 1960a,b).

The *degree of welding* in tuffs described in this report is based on flattening of pumices in hand specimens and flattening of pumice and shards in thin section. These criteria describe the degree to which pyroclasts have undergone plastic deformation during compaction of the tuff. Strickly speaking, *welding* refers to the fusing together of adjacent pyroclasts in a cooling ash-flow sheet (Smith, 1960b). Nevertheless, as used in this report *welding* is a common and useful field term that differentiates between tuffs that are uncompacted and porous and tuffs that are compacted and less porous. [This terminology was adopted and slightly modified from that of Peterson (1979).] Ignimbrites in which pumice lapilli show no flattening are called *nonwelded*. Ignimbrites with aspect ratios of 1.5:1 to 2:1 are termed *partly* or *partially welded*; those with aspect ratios of 2:1 to 6:1 are *moderately welded;* and those with aspect ratios >6:1 are *densely welded*.

Otowi Member

The exposed portion of the Otowi Member of the Bandelier Tuff in Los Alamos Canyon is a simple cooling unit made up of nonwelded, vitric ignimbrite. This poorly indurated tuff crops out in shallow drainages that incise gentle colluvial-covered slopes on the canyon floor. Bedding or parting features are absent in the exposed portions of the Otowi Member, suggesting that the upper part of this ash-flow sheet is a single, thick, ash-flow deposit. The exposed portion of the Otowi Member is 18 to 21 m thick above the canyon floor, and an additional 47 m (including the Guaje Pumice Bed) was penetrated at water-supply well Otowi 4 (Stoker *et al.*, 1992). Therefore, the total thickness of this unit is ~67 m in the vicinity of borehole Otowi-4 (Fig. 1). Borehole LADP-4 in DP Canyon penetrated 85 m of Otowi Member, including 8.5 m of the basal Guaje Pumice Bed.

The Otowi Member consists of light-gray to pinkish-orange pumice lapilli supported by a white-to-tan, ashy matrix. The matrix is made up of glass shards, broken pumice fragments, phenocrysts, and fragments of nonvesiculated perlite. Glass shards are glassy and clear, showing no evidence for either post-emplacement high-temperature devitrification or subsequent low-temperature diagenetic alteration. Pumice lapilli typically make up 10 to 30% of the tuff, are equant to subequant (aspect ratios = 1:1 to 2:1), and range from 0.5 to 6 cm in diameter. Pumices are larger (up to 20 cm) and more abundant (~40% of the rock) at the top of the Otowi Member. These pumices have a vitreous luster on fresh surfaces, and the excellent preservation of delicate tubular vesicles imparts a fibrous appearance. Pumice and matrix materials acquire a pinkish-orange coloration near the top of the unit. This coloration may be the result of either the oxidation of iron by escaping vapors as the ash-flow sheet cooled or incipient weathering of the top of the unit before deposition of overlying units.

Two bulk-rock samples of Otowi Member contain 7 to 9% phenocrysts of quartz and sanidine 0.5 to 2 mm in diameter (Table II, Fig. 2). Clinopyroxene, plagioclase, and hornblende are present in trace amounts; the plagioclase and hornblende may be xenocrysts. Accessory minerals include magnetite, zircon, and an as-yet-unidentified rare-earth silicate. In thin section, the rare-earth accessory mineral is stubby and has the weak-to-moderate pleochroism characteristic of allanite; however, other grains are lath-like and completely absorb light length-wise like perrierite or chevkinite.

The upper part of the Otowi Member contains 2 to 5% chocolate-brown to black lithics derived from intermediate-composition lava flows. These lithics are 0.3 to 3 cm in diameter and consist primarily of aphanitic dacite. Phenocryst-rich dacites derived from the Tschicoma Formation form a subordinate lithic assemblage.

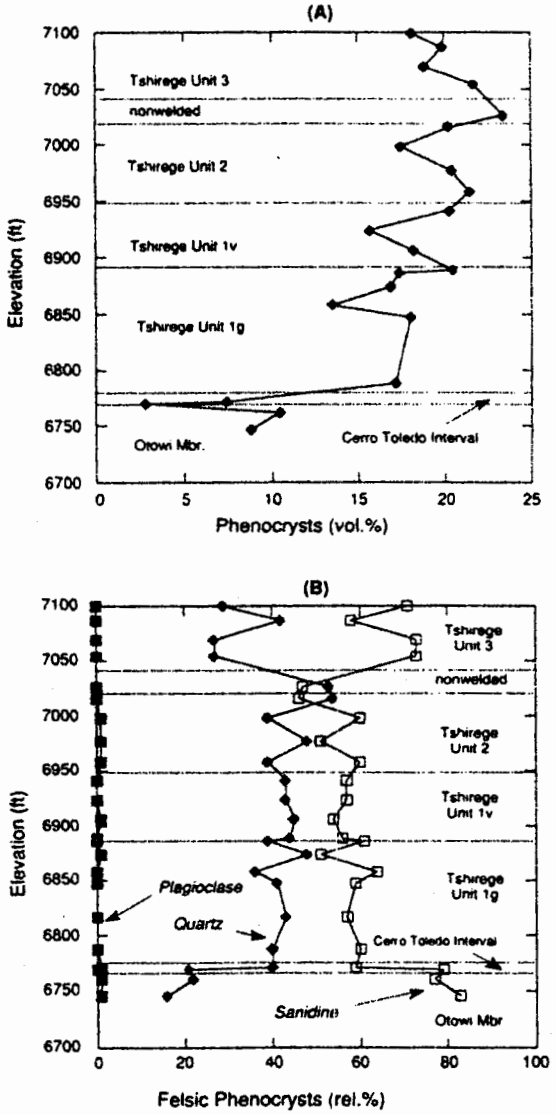

Fig. 2. Variation diagrams of phenocryst abundances in thin section for samples collected in stratigraphic section OU-1106-STRAT2. (A) Variations in total phenocryst abundances are shown on a void-free basis but are not corrected for porosity variations in the tuffs. (B) Variations in the relative proportions of the felsic phenocrysts.

Cerro Toledo Interval

The Cerro Toledo interval is an informal name given to a sequence of epiclastic sediments and tephras of mixed provenance that lie between the two members of the Bandelier Tuff. This unit contains deposits normally assigned to the Cerro Toledo Rhyolite (Smith *et al.*, 1970), including well-stratified tuffaceous sandstones and siltstones as well as primary ash-fall and pumice-fall deposits. The Cerro Toledo interval at TA-21 also contains intercalated deposits not normally assigned to the Cerro Toledo Rhyolite; these include poorly sorted sand, gravel, cobble, and boulder deposits derived from lava flows of the Tschicoma Formation. The Cerro Toledo interval is ~3 m thick at OU-1106-STRAT1 and OU-1106-STRAT2 and 9 m thick at OU-1106-STRAT3. In LADP-4, the Cerro Toledo interval is 12 m thick. These deposits also crop out in Los Alamos Canyon at TA-41 west of TA-21, in DP Canyon east of DP Spring, and in Pueblo Canyon north of TA-21. The distribution is widespread throughout the area; however, predicting the presence and thickness of these deposits is problematic because of the nature of fluvial systems.

Rhyolitic tuffaceous sediments and tephras are the dominant lithologies found in the Cerro Toledo interval at the three stratigraphic sections examined in this study. The tuffaceous sediments are the reworked equivalents of Cerro Toledo Rhyolite tephras erupted from the Cerro Toledo and Rabbit Mountain rhyolite domes located in the Sierra de los Valles. Because of their poorly consolidated nature and the steep topography on which they were deposited, these tephras were quickly eroded from the highlands to the west, transported by east-flowing stream systems, and deposited within a lowland area that is now the site of the Pajarito Plateau. These reworked tephras are subdivided into subunits on Plate 2 based on bedding characteristics, composition of clasts, and mode of deposition. Normally, these subunits pinch out laterally and can not be correlated over wide areas. Individual subunits are 5 to 175 cm thick and generally have well-defined stratification imparted by grading and sorting of ash- to block-sized clasts. Bedding characteristics include graded bedding, cross

TABLE II

MODAL PETROGRAPHY OF TUFFS AT TA-21

TABLE II

MODAL PETROGRAPHY OF TUFFS AT TA-21

Field Number	OU-1106-STRAT2-1	OU-1106-STRAT2-2	OU-1106-STRAT2-3	OU-1106-STRAT2-4	OU-1106-STRAT2-5	OU-1106-STRAT2-6	OU-1106-STRAT2-7	OU-1106-STRAT2-9
Site Identification	160	161	162	163	164	165	166	200
Stratigraphic Unit	Otowi Mbr	Otowi Mbr	Cerro Toledo Interval	Cerro Toledo Interval	Tshirege Mbr. (1g)	Tshirege Mbr (1g[d]	Tshirege Mbr (1g)	Tshirege Mbr. (1g)
Lithology[a]	nwt	nwt	b	b	nwt	Single Hb. pumice	nwt	nwt
Major Alteration[b]	GI	GI	GI	GI	GI	GI	GI	GI
Minor Alteration[b]	--	--	--	--	--	--	--	--
Matrix Materials (vol. %) [c]								
Ash, shards, pumice	85.9	87.5	94.1	86.9	80.6	59.1	96.5	79.6
Lithics (silicic volcanics)	3.6	0.6	1.5	2.0	0.8		0.8	1.2
Lithics (intermediate lavas)	1.2	0.1	1.4	1.0	0.05	0.1	--	0.2
Lithics (other)	0.1 (granitic)	0.1 (granitic)	--	--	0.1 (granitic)	--	--	-
Granophyric pumice	--	--	--	--	--	--	--	
Perlitic glass fragments	0.5	0.3	0.4	2.4	1.0	--	0.2	1.1
Phenocrysts (vol. %) [c]								
Quartz	1.4	2.2	0.6	3.0	6.7	0	1.1	7.2
Alkali Feldspar	7.2	8.0	2.1	4.3	10.0	3.1	1.4	10.5
Plagioclase	0.04 (3)	0.1 (2)	-	0.05 (2)	0.1 (1)	31.8	--	0.04 (2)
Biotite			0 (1)	-	-	0 (1)	-	0 (2)
Hornblende	0 (3)	--			0 (7)	4.9	-	0 (5)
Orthopyroxene		-		-		0 (3)		
Clinopyroxene	0.1 (16)	0.04 (11)	0 (2)	0.05 (9)	0.2 (18)	0.6	0.04 (6)	0.2 (15)
Fayalite		-	--	-	--	--	--	
Other (Psuedo-morphs ect.)	--	-	--	-	--	0.4 (sanidine over growths on plagioclase)	-	-
Accessory Minerals (counts) [c]								
Fe Ti Oxides	2 (39)	1 (17)	0 (2)	3 (9)	2 (32)	2 (13)	0 (6)	1 (12)
Pemente/Chevkinite/Allanite	-	0 (1)	0 (2)	0 (1)	--		-	--
Zircon	0 (3)	0 (6)	0 (1)	0 (3)	0 (1)	0 (1)	--	-
Sphene	-	-	--	-	--	--	--	--
Total Counts	2799	2475	5132	6057	2779	2982	4755	2414
Voids (counts)	415	421	1507	1676	189	826	2104	167
Remarks	Thin hematite rims around magnetite	Thin hematite rims around magnetite				Hematite after magnetite		
Phenocryst Summary								
% Phenocrysts (Void free)	8.7	10.3	2.7	7.4	17.0	40.8	2.5	17.9
Quartz as % of Felsic Phenos	16	22	21	40	40	0	43	41
Sanidine as % of Felsic Phenos.	83	77	79	59	60	9	57	59
Plagioclase as % of Felsic Phenos.	1	1	0	1	0	91	0	0

[a] *Lithology: nwt = nonwelded ash-flow tuff; pwt = partially-welded ash-flow tuff; mwt = moderately-welded ash flow tuff; b= bedded tuff, includes pumice falls and stratified reworked deposits*

[b] *Alteration: GI = none, original volcanic glass preserved; D = high-temperature devitrification; VP = vapor-phase alteration.*

[c] *Matrix materials and phenocrysts are presented as volume percent concentrations on a void-free basis. Accessory minerals are shown as the number of grains counted in the point count. The number in parentheses is a visual countof all grains of a component observed in a thin section.*

[d] *This thin section contains highly vesiculated pumice, some of which were plucked during sample preparation. The low phenocryst content is an artifact of sample and preparation, and it is not representative of the Tshirege Member.*

TABLE II

MODAL PETROGRAPHY OF TUFFS AT TA-21 (CONT)

Field Number	OU-1106-STRAT2-10	OU-1106-STRAT2-11	OU-1106-STRAT2-12	OU-1106-STRAT2-13	OU-1106-STRAT2-14	OU-1106-STRAT2-15	OU-1106-STRAT2-16	OU-1106-STRAT2-17
Site Identification	201	202	203	204	205	206	432	436
Stratigraphic Unit	Tshirege Mbr. (1g)	Tshirege Mbr. (1g)	Tshirege Mbr. (1g)	Tshirege (1g)	Tshirege Mbr. (1v)	Tshirege Mbr. (1v)	Tshirege Mbr. (1v)	Tshirege Mbr. (2)
Lithology[a]	nwt	nwt	nwt	nwt	nwt	nwt	nwt	pwt
Major Alteration[b]	Gl	Gl	Gl	D	D	D	VP, D	VP, D
Minor Alteration[b]	--	--	D	Gl	--	VP	--	--
Matrix Materials (vol. %) [c]								
Ash, shards, pumice	83.8	80.7	87.4	77.1	81.2	66.8	64.7	63.6
Lithics (silicic volcanics)	2.1	0.5	1.2	1.8	0.5	14.3	0.4	0.4
Lithics (intermediate lavas)	0.2	0.2	1	0.3	0.1	0.6	0.7	0.7
Lithics (other)	--	--	--	--	--	--	-	0.04 (granophyre)
Granophyric pumice	--	--	--	--	--	2.4	13.9	13.7
Perlitic glass fragments	0.3	1.6	1.2	0.5	--	--	--	--
Phenocrysts (vol. %) [c]								
Quartz	4.8	7.9	7.0	8.8	8.1	6.8	8.5	8.2
Alkali Feldspar	8.6	8.4	11.0	11.1	9.7	8.8	11.3	12.6
Plagioclase	0.04 (1)	0.2 (3)	0 (2)	0.04 (3)	0.1 (8)	--	0 (5)	0.1
Biotite	0 (1)	0 (1)	--	--	--	--	0 (5)	--
Hornblende	0.04 (5)	0 (3)	0.1 (3)	0 (1)	0.04 (8)	0.04 (5)	0.04 (3)	0.1 (6)
Orthopyroxene	--	--	--	--	-	--	--	--
Clinopyroxene	0 (15)	0.1 (15)	0.2 (17)	0.3 (9)	0.1 (4)	--	--	0.2 (4)
Fayalite	--	0.1 (1)	--	0.1 (2)	0.1 (2)	0 (1)	0.04 (1)	
Other (Pseudomorphs ect.)	--	0.1 (aggregates of secondary opaques)	0.1 (aggregates of secondary opaques)	0.1 (aggregates of secondary opaques)	--	--	0.3 cpx?	0.2 fayalite?
Accessory Minerals (counts) [c]								
Fe-Ti Oxides	2 (30)	2 (23)	2 (31)	1(28)	1(45)	1 (45)	1 (23)	3
Perrierite/Allanite	--	0 (1)	-	--	--	0 (1)	0 (1)	--
Zircon	-	--	0 (4)	0 (2)	0 (3)	0 (5)	0 (6)	0 (4)
Sphene	-	--	--	--	-	-	-	--
Total Counts	2701	2781	2785	2868	2855	2364	2374	2929
Voids (counts)	362	543	361	317	372	169	109	126
Remarks		Thin hematite rims around magnetite; pumices glassy but shardy matrix partly devitrified	Thin hematite rims around magnetite; pumices glassy but shardy matrix partly devitrified	Hematite rims around magnetite ; pumices partly glassy; shardy matrix devitrified	Hematite after magnetite	Hematite after magnetite	Hematite after magnetite	Hematite after magnetite
Phenocryst Summary								
% Phenocrysts (Void free)	13.4	16.8	17.4	20.4	18.1	15.6	20.2	21.4
Quartz as % of Felsic Phenos.	36	48	39	44	45	43	43	39
Sanidine as % of Felsic Phenos.	64	51	61	56	54	57	57	60
Plagioclase as % of Felsic Phenos.	0	1	0	0	1	0	0	1

[a] Lithology: nwt = nonwelded ash-flow tuff, pwt = partially welded ash-flow tuff; mwt = moderately-welded ash flow tuff; bs= bedded tuff, includes pumice falls and stratified reworked deposits

[b] Alteration: Gl = some original volcanic glass preserved, D = [illegible] devitrification, VP = [illegible] alteration

[c] Matrix materials and phenocrysts are presented as volume percent concentrations [illegible] Accessory minerals are shown as the number of grains counted in the point count. The number in parenthesis [illegible]

TABLE II

MODAL PETROGRAPHY OF TUFFS AT TA-21 (CONT)

OP - HIGH-OUT - USA

[a] Lithology: nwt = nonwelded ash-flow tuff; pwt = partially welded ash-flow tuff; mwt = moderately welded ash-flow tuff; bs = bedded tuff, includes pumice falls and [illegible]

[b] Alteration: Gl = none, original volcanic glass preserved, D = high temperature devitrification, VP = vapor-phase alteration

[c] Matrix materials and phenocrysts are presented as volume percent concentrations on a void free basis. Accessory minerals are shown as the number of grains counted in the point count. The number in parentheses is a visual count of all grains of a component observed in a thin section

TABLE II

MODAL PETROGRAPHY OF TUFFS AT TA-21 (CONT)

Field Number	OU 1106 STRAT2 18	OU 1106 STRAT2 19	OU 1106 STRAT2 20	OU 1106 STRAT2 21	OU 1106 STRAT2 22	OU 1106 STRAT2 23	OU 1106 STRAT2 24	OU 1106 STRAT2 25
Site Identification	439	440	440	440	440	440	440	440
Stratigraphic Unit	Tshirege Mbr (2)	Tshirege Mbr (2)	Tshirege Mbr (2)	Tshirege Mbr (nw)	Tshirege Mbr (3)	Tshirege Mbr (3)	Tshirege Mbr (3)	Tshirege Mbr (3)
Lithology[a]	mwt	mwt	mwt	nwt	nwt	nwt	pwt	pwt
Major Alteration[b]	VP, D	VP, D	VP, D	VP, D	VP, D	VP, D	VP, D	VP, D
Minor Alteration[b]	-	-	-	-	-	-	-	-
Matrix Materials (vol. %) [c]								
Ash, shards, pumice	70.8	71.3	70.5	67.4	73.3	76.4	74.7	69.3
Lithics (silicic volcanics)	0.2	2.9	0.1	0.4	0.4	0.6	0.7	0.4
Lithics (intermediate lavas)		0.03	..	0.5	..	0.6	0.6	0.3
Lithics (other)			..	-	0.1 metamorphic	0.03 plutonic/meta	-	-
Granophyric pumice	8.5	8.3	9.4			3.6	4.3	4.5
Perlitic glass fragments				..	-	..	-	-
Phenocrysts (vol. %) [c]								
Quartz	9.7	6.7	10.6	12.0	5.9	5.0	8.1	5.0
Alkali Feldspar	10.3	10.4	9.1	10.7	15.8	13.4	11.1	12.1
Plagioclase	0.2 (5)	0.2 (4)	0.1 (2)	0.1 (2)	0.03 (1)	0.03 (2)	0.1 (3)	0.1 (3)
Biotite	0 (2)		0.1 (6)	..		..		
Hornblende	0.03 (6)	0.03 (8)	0.1 (2)	0.1 (4)	0.03 (9)	0 (5)	0.1 (5)	0.03 (5)
Orthopyroxene			-	0 (2)?	-	0.2 (12)		
Clinopyroxene	0 (2)				0.03		0.4 (21)	0.4 (30)
Fayalite				-	-			
Other (Pseudomorphs ect.)	0.1 (5) fayalite?	0.1 fayalite?	0.2 fayalite?	0.2 fayalite?		0.03 (4) cpx?		
Accessory Minerals (counts) [c]								
Fe-Ti Oxides	2	2	2	2	1	1	3	6
Perrierite-Chevkinite-Allanite		0 (3)			0 (6)	0 (3)	0	0 (4)
Zircon	0 (1)	0 (10)	0 (6)	0 (10)	0 (4)	0 (8)	0 (8)	0 (8)
Sphene			0 (several grains)	-	0 (10)	0 (19)		
Total Counts	3278	3275	2558	3349	3093	2933	3331	3157
Voids (counts)	61	67	13	283	210	107	121	193
Remarks	Hematite after magnetite	Hematite after magnetite	Hematite after magnetite	Hematite after magnetite	Hematite after magnetite	Hematite after magnetite	Hematite after magnetite	Hematite after magnetite
Phenocryst Summary								
% Phenocrysts (Void free)	20.3	17.4	20.2	23.1	21.7	18.5	19.8	18.1
Quartz as % of Felsic Phenos	48	39	54	53	27	27	42	29
Sanidine as % of Felsic Phenos	51	60	46	47	73	73	58	71
Plagioclase as % of Felsic Phenos	1	1	0	0	0	0	0	0

[a] Lithology: nwt = nonwelded ash flow tuff, pwt = partially welded ash-flow tuff, mwt = moderately-welded ash-flow tuff, bs = bedded tuff, includes pumice falls and stratified reworked deposits

[b] Alteration: Gl = none, original volcanic glass preserved, D = high temperature devitrification, VP = vapor phase alteration

[c] Matrix materials and phenocrysts are presented as volume percent concentrations on a void free basis. Accessory minerals are shown as the number of grains counted in the point count. The number in parentheses is a visual count of all grains of a component observed in a thin section

bedding, and planar bedding (Fig. 1 of Goff, Sec. II, this report). Orange oxidation and clay-rich horizons suggest that at least two periods of soil development are recorded within the Cerro Toledo deposits. These soils are clay-rich and may act as barriers to the downward movement of vadose zone groundwater.

Some of the epiclastic tuffaceous deposits contain both crystal-poor and crystal-rich varieties of pumice. The ashy matrix of these deposits is commonly crystal-rich and contains subhedral sanidine and quartz up to 2 mm in diameter. The mixed pumice populations and the crystal-rich nature of the matrix suggest that these reworked tuffs were derived from both the Cerro Toledo Rhyolite and the underlying Otowi Member.

The tuffaceous portion of the Cerro Toledo interval also contains primary fall deposits. In the lower part of the unit, fall deposits contain <3% phenocrysts of <0.2-mm sanidine and quartz (Table II, Fig. 2). These crystal-poor tephras are equivalent to the Cerro Toledo Rhyolite described by Heiken *et al.* (1986). Primary pumice falls in the upper part of the Cerro Toledo interval contain >7% phenocrysts of >1-mm sanidine and quartz. The petrographic characteristics are similar to those found in the overlying Tshirege Member. However, a clay-rich soil horizon at the top of the Cerro Toledo sequence suggests that these deposits were exposed at the surface for a substantial period of time before deposition of the overlying Tshirege Member. The primary pumice falls in the Cerro Toledo interval may be useful time-stratigraphic markers for correlating deposits over widespread areas of the Pajarito Plateau, but additional work is required to establish correlations between individual tephras. The pumice falls tend to form the most porous and permeable horizons within the Cerro Toledo interval, and locally they may provide important pathways for moisture transport in the vadose zone.

A subordinate lithology within the Cerro Toledo interval includes clast-supported gravel, cobble, and boulder deposits made up of porphyritic dacite derived from the Tschicoma Formation. These dacitic epiclastic deposits are interbedded with the tuffaceous rocks. The coarse dacitic deposits are typically 0.25 to 1.2 m thick, and they generally occur as overlapping lenticular paleochannels up to 1 m deep. In some places, cobbles of densely welded, crystal-rich Otowi ignimbrite are also present. At OU-1106-STRAT1, cobbles and boulders derived from Tschicoma lava flows occur in a matrix of reworked pumice and ash, filling a paleochannel that cut 0.8 m into the underlying Otowi Member. At OU-1106-STRAT3, a paleochannel in the middle of the Cerro Toledo interval contains Tschicoma boulders up to 1 m in diameter.

It is important to note that the proportion of tuffaceous to dacitic detritus making up deposits at this stratigraphic horizon varies from location to location across the Pajarito Plateau. Whereas Cerro Toledo deposits described in this report are dominantly tuffaceous in character, rocks at this stratigraphic horizon in lower DP Canyon (Goff, Sec. II, this report) and in the subsurface at TA-55 (Gardner *et al.* 1993) consist predominantly of coarse dacitic detritus derived from the Tschicoma Formation and include only subordinant amounts of interbedded tuffaceous detritus. The coarse dacitic deposits in the Cerro Toledo horizon are similar to those found in the Puye Formation, a volcanic fanglomerate that lies beneath the Otowi Member. The similarity of Cerro Toledo deposits to those of the Puye Formation and the mixed provenance of the detritus within these deposits indicates that Puye-like alluvial fans continued to develop on the east side of the Jemez Mountains after deposition of the Otowi Member and during the period of Cerro Toledo volcanic activity.

Tshirege Member

The Tshirege Member is a multiple-flow ash-flow sheet that forms the prominent cliffs at TA-21. It is a compound cooling unit whose physical properties vary vertically and laterally. Variations in physical properties result from zonal patterns of welding and crystallization determined by emplacement temperature, thickness, gas content, and composition (Smith, 1960a,b). The thickness of this unit ranges from 89 to 98 m in the three sections measured. All but the uppermost unit (unit 4) of the Tshirege Member occur at TA-21.

Previous workers identified mappable subunits in the Tshirege Member based on a combination of surface-weathering patterns, welding features, and crystallization characteristics (Baltz *et al.*, 1963; Weir and Purtymun, 1962; Crowe *et al.*, 1978; Vaniman and Wohletz, 1990, 1991). Figure 3 correlates the stratigraphic units used by these earlier workers. A certain amount of confusion has resulted from inconsistent use of unit names for the Tshirege Member. In part, this confusion occurs because different criteria were used by different workers to identify the units. But equally important, the differences in nomenclature arose because the internal stratigraphy of the Tshirege Member varies laterally as a function of distance from the caldera source.

This paper generally follows the stratigraphic nomenclature of Vaniman and Wohletz (1990,1991) to describe subunits of the Tshirege Member because their geologic map overlaps the western end of TA-21. However, we do deviate from their nomenclature in two respects. First, we include their nonwelded unit below unit 2 as part of unit 1v because all tuffs below unit 2 are nonwelded. Second, we define unit 1v as a lower resistant orange-

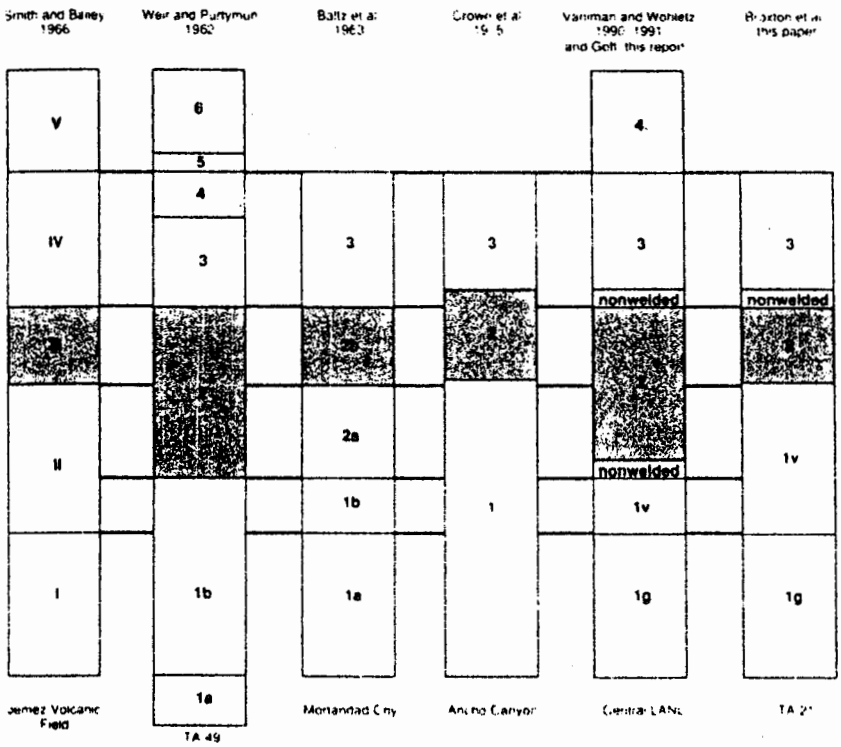

Fig. 3. Stratigraphic nomenclature for the Tshirege Member as used in this report correlated to that of other investigators working on the Pajarito Plateau.

brown colonnade tuff overlain by an upper slope-forming light-colored nonwelded tuff. Vaniman and Wohletz (1990, 1991) considered the upper-slope-forming, light-colored nonwelded tuff as part of unit 2. We believe the Tshirege nomenclature used in this report better reflects the presence of three distinct cooling units in this compound cooling unit at this location. Earth scientists for the ER program are presently conducting stratigraphic studies on the Pajarito Plateau to resolve differences between the different systems of stratigraphic nomenclature used by Los Alamos ER investigators.

Tsankawi Pumice Bed. The Tsankawi Pumice Bed is the basal pumice fall of the Tshirege Member (see Fig. 2, Goff, Sec. II, this report). This pumice bed is 73 to 95 cm thick where exposed and consists of two subunits, each of which has normally graded bedding. The lower subunit is 60 to 74 cm thick and contains equant, angular to subangular clast-supported pumice lapilli up to 6-cm diameter. Pumices are typically fibrous with a vitreous luster. Coarse ash and abundant phenocrysts make up the matrix. A 2- to 7-cm-thick ash bed made up of fragmented pumice, ash, and crystals overlies the lower pumice bed. The upper pumice bed is 13 to 14 cm thick and consists of clast-supported pumice lapilli that grade upwards into a coarse ash bed at the top of the unit.

Pumices in the Tsankawi Pumice Bed are rhyolitic in composition and contain ~5% phenocrysts. Phenocrysts consist of 0.2- to 2-mm sanidine and quartz. There is also a small (<5%) population of medium-gray, dense, finely vesiculated dacitic hornblende-bearing pumice in the Tsankawi Pumice Bed. In addition to hornblende, these finely vesiculated pumices contain clinopyroxene and small subhedral grains of plagioclase. These hornblende-bearing pumices are a diagnostic feature of the Tsankawi Pumice Bed and overlying ash-flow units (Bailey *et al.*, 1969). Lithics make up 1 to 2 % of these pumice beds and consist of dark-gray to dark-red clasts derived from porphyritic dacite. Lithics are 0.5 to 4 cm in diameter.

Tshirege Unit 1g. Unit 1g is the lowermost unit in the thick ignimbrite deposit of the Tshirege Member. This 22- to 32-m-thick unit is poorly indurated but commonly forms near-vertical cliffs because a prominent resistant bench occurs at the top of the unit, forming a protective cap over softer, underlying tuffs.

Fresh tuff surfaces are light-gray to white at the base of the unit but gradually become light pink-orange 9 to 12 m above the base. This color change becomes more pronounced upsection and coincides with the tuffs becoming more resistant to erosion. The uppermost part of unit 1g is a resistant, cliff-forming tuff, the top of which forms a nearly-flat-lying bench up to several meters wide locally. The hardness of these uppermost tuffs may be the result of incipient welding or incipient devitrification near the top of the unit. The bench at the top of the unit marks the base of the vapor-phase notch (Crowe *et al.*, 1978) which is discussed in more detail below. Outcrop surfaces in unit 1g typically weather to a pale-orange color. Weathered cliff faces have a distinctive swiss-cheese appearance because large holes penetrate case-hardened cliff faces and expose the soft underlying tuffs to wind and water erosion.

Unit 1g is a nonwelded, poorly sorted, vitric ignimbrite. It consists of light-gray, vitreous, crystal-rich pumice lapilli supported by a matrix of coarse ash, shards, pumice fragments, and abundant sanidine and quartz phenocrysts. As observed in thin section, delicate glass shards are clear and perfectly preserved and show no evidence of secondary alteration. Glass in the shards is tan to brown in tuffs just below the vapor-phase notch. Pumice lapilli typically make up 30 to 50% of the rock. These lapilli are commonly equant and fibrous, and they are 2 to 5 cm in diameter. Locally, pumice clasts are up to

14 cm in diameter. Most pumices are rhyolitic in composition, but dacitic hornblende-bearing pumices also occur in small amounts.

A distinctive pumice-poor surge deposit forms the base of this unit. This surge bed is 10 to 25 cm thick and contains undulating, laminated, dune-like beds. These surge deposits consist of coarse ash and abundant broken crystals. Individual beds in this unit are 0.5 to 9 cm thick. Some of the surge beds have low-angle cross beds in which laminations are 1 to 30 mm thick and have normal grading. The undulating tops for some of these surge deposits have wavelengths of up to 4 m. The surge deposit is overlain by a thick ignimbrite that makes up the remainder of the unit. The lower 0.3 to 0.7 m of this ignimbrite is an ash-rich tuff that grades upwards into the main body of the deposit, which consists of nonstratified tuff containing abundant pumice lapilli and blocks. This ignimbrite was probably deposited by the passage of a single, large ash flow.

Phenocrysts make up 12 to 16% of unit 1g (Table II, Fig. 2). Sanidine and quartz make up >98% of the phenocryst assemblage, and the maximum size is 2 to 3 mm. Clinopyroxene, hornblende, and fayalite are the dominant ferromagnesian minerals; magnetite, zircon, and perrierite/chevkinite/allanite are accessory minerals. Most of the hornblende and plagioclase identified during point counts of bulk rock samples are associated with a dacitic hornblende-bearing pumice similar to that found in the Tsankawi Pumice Bed. The remainder of the hornblende and plagioclase occurs in the tuff matrix and probably was derived from disaggregation of hornblende-bearing pumice during emplacement. One particularly large hornblende-bearing pumice was thin-sectioned and point-counted (Table II; sample OU-1106-STRAT2-6). Phenocrysts, making up 41% of this pumice, consist of hornblende, plagioclase, clinopyroxene, orthopyroxene, and minor sanidine; accessory minerals include magnetite and zircon.

Lithics are typically sparse (<1%) in unit 1g. Lithic clasts are usually reddish-brown-to-black porphyritic dacite and crystal-poor, devitrified welded tuffs. Rare granitic lithics also occur in these tuffs. Most lithics are 0.2 to 5 cm in diameter.

Tshirege Unit 1v. Unit 1v forms a combination of cliff-like and sloping outcrops that separates the resistant bench at the top of unit 1g from the near-vertical cliff of unit 2 (see Fig. 3 of Goff; Sec. II, this report). The base of unit 1v is a resistant orange-brown colonnade tuff that overlies the bench at the top of unit 1g. This colonnade tuff forms a 1- to 3-m-thick cliff that has distinctive columnar jointing. These features suggest the colonnade tuff may be slightly welded, although pumices show no discernable compaction at hand-specimen scale. The colonnade tuff is overlain by slope-forming tuffs that make up the bulk of unit 1v. These slope-forming tuffs form a distinctive white band of outcrops sandwiched between the darker colored outcrops of the colonnade tuff and unit 2. The light-colored tuffs lack discernable bedding or parting features at TA-21, but these features are present in other locations and indicate the presence of multiple flow units. The upper contact of unit 1v corresponds to the abrupt transition from light-colored, nonwelded, slope-forming tuffs to the darker, partially welded, cliff-forming tuffs of unit 2. At locations east of TA-21 (for example, at TA-54), thin but well-defined surge beds mark the contact between units 1v and 2. These surge beds are absent at TA-21. Unit 1v thickens eastward from 16 to 20 m at TA-21.

Unit 1v is a nonwelded, poorly sorted, devitrified ignimbrite. It consists of tubular, crystal-rich pumice lapilli supported by a light-gray-to-white ashy matrix of shards, pumice fragments, and abundant phenocrysts. Relict shards occur in a cryptocrystalline groundmass. Pumice lapilli typically make up 30 to 50% of the rock and are 0.2 to

6 cm in diameter. Pumices are chocolate-brown to dark purple-gray in the lower colonnade tuff and grade upwards into a light-gray to medium-gray color in the overlying white tuffs. Pumice color variations correspond with mineralogical changes that accompany increasing vapor-phase alteration upsection. Cristobalite is the dominant secondary silica mineral in the colonnade tuff whereas tridymite is more common in the white tuffs. Pumice lapilli typically have a sugary texture as a result of more intense vapor-phase crystallization in the upper part of the unit. Much of the original vesicular structure of pumices is preserved in hand samples. However, on the microscopic scale, most of the fine structure in pumices is destroyed by devitrification and vapor-phase crystallization. Overlapping spherulites, octahedral cristobalite, and lath-like tridymite (in the upper part of the unit) replace the original volcanic glass in the pumices. The colonnade tuff has a pock-marked appearance because of the selective weathering of soft pumice from the enclosing more resistant matrix.

The vapor-phase notch at the base of this unit is a thin, horizontal zone of preferential weathering that forms a widespread mappable marker horizon throughout the Pajarito Plateau. There is no depositional break associated with the vapor-phase notch at TA-21 or at other localities. The abrupt transition from vitric tuffs below the notch to devitrified tuffs above suggests that this feature is

TABLE III

Lithologic Characteristics of the Vapor-Phase Notch in Stratigraphic Section OU-1106-STRAT2 at TA-21

	Tuffs Immediately Below Notch	Tuffs in the Vapor-Phase Notch	Tuffs Immediately Above Notch
Pumice	Original glass in pumice disappears rapidly upward, pumices make up ~50% of rock, size 0.2 to 9 cm	Original volcanic glass mostly destroyed by devitrification; sugary texture; size 0.2 to 4 cm	Devitrified relict pumice makes up ~50% rock, sugary texture, 0.2 to 6 cm, no visible compaction but may be slightly welded.
Matrix	Small fragments of vitric pumice, pale, peach-colored, crystal rich, devitrified ashy matrix	White, fine-grain, devitrified ash, relict small pumice fragments, and phenocrysts, most original textures destroyed	Fine-grain, devitrified, crystal-rich ash, relict small pumice fragments, texture of small pumice fragments well preserved
Lithics	Dark-gray and -brown porphyritic and aphanitic lavas, ~3% of rock, size 0.5 to 6 cm	Light-gray lavas, and black obsidian, ~3% of rock; size 0.5 to 2 cm	Light-gray lavas abundance varies vertically from 1 to 5%, size 0.5 to 5 cm
Color on Fresh Surfaces	Pale pink to orange grading up to dark orange.	Light-gray with pink hue, wispy areas of dark orange	White and pink matrix, chocolate-brown and dark-gray pumices
Weathering Characteristics	Grades up from white, poorly indurated tuffs that form rounded outcrops to orange, resistant bench, large "pot" holes, where case-hardened surface penetrated by erosion, pumice more resistant to erosion than matrix, lacks fractures.	Soft, horizontal, preferentially eroded recess in rock defined by alignment of 1.5-m-tall flattened caves; sometimes forms bench several meters wide, fractures from above terminate abruptly in this zone	Colonnade resistant tuff; orange-brown outcrops, distinctive "pockmarked" surfaces from selective erosion of soft, altered pumice

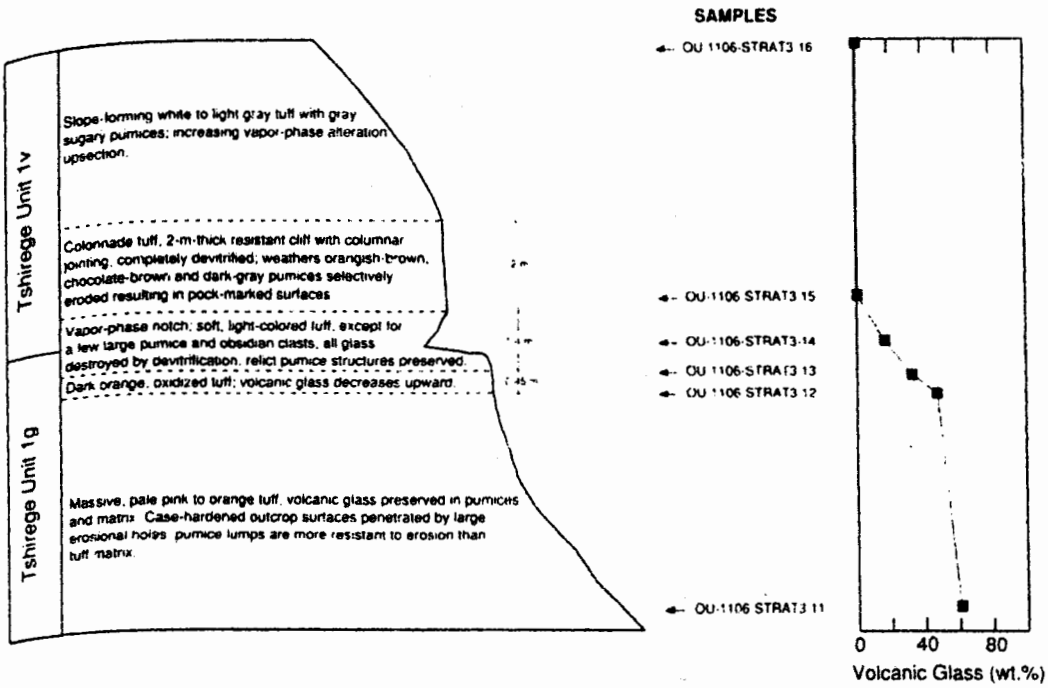

Fig. 4. Detail of lithologic changes across the vapor-phase notch in stratigraphic section OU-1106-STRAT3 at TA-21. The vapor-phase notch marks the rapid transition from vitric tuffs below to devitrified and vapor-phase altered tuffs above. Volcanic glass is the most abundant constituent in tuffs of unit 1g, but disappears abruptly upsection over a 2 m interval within the vapor-phase notch. The contact between units 1g and 1v is arbitrary chosen as the first occurrence of volcanic glass as one moves downsection through the vapor-phase notch interval.

the base of the devitrification that occurred in the hot interior of the cooling ash-flow sheet after emplacement. Initially, primary volcanic glass was deposited within all parts of the Tshirege Member, but high heat retention and outgassing of volatiles caused all of the glass above the vapor-phase notch to crystallize to alkali feldspar and silica polymorphs. Table III and Fig. 4 summarize the principal lithological and mineralogical characteristics of the vapor-phase notch.

Phenocryst assemblages and abundances are similar to those in unit 1g (Table II, Fig. 2). Ferromagnesian phenocrysts show increasing degrees of oxidation up section. Fayalite is more common than in unit 1g. Lithic clasts make up 1 to 5% of the tuff near the base of the unit but decrease to <1% in the upper part. Most lithics are 0.5 to 5 cm in diameter and are similar to those described for unit 1g.

Near-vertical fractures penetrate the tuffs in unit 1v. These fractures appear to be downward extensions of prominent fractures in unit 2. Some of the fractures penetrate across the vapor-phase notch before dying out in the softer tuffs of unit 1g.

Tshirege Unit 2. Unit 2 is the 25- to 27-m-thick, vertical cliff-forming unit in the Tshirege Member at TA-21. The first appearance of unconsolidated nonwelded tuffs on the broad bench on top of unit 2 defines its upper contact. This unit forms a distinctive, medium-brown, vertical cliff that stands out in marked contrast to the slope-forming, lighter colored tuffs above and below (see Fig. 3 of Goff; Sec II, this report). This unit is the zone of greatest welding in the Tshirege Member at TA-21, and its thickness decreases from 21 to 10 m eastward.

Unit 2 is a poorly sorted, vapor-phase-altered ignimbrite. The tuffs consist of relatively sparse, crystal-rich pumice lapilli supported by an ashy matrix of shards, pumice fragments, and abundant phenocrysts. The compaction of pyroclasts in the tuff increases upsection and is greatest in the upper part of the unit. The tuff matrix is light pinkish-tan to light-purplish-gray, and the degree of coloration increases with increased welding. Pumice lapilli are medium-gray to grayish-brown in color and have aspect ratios of 1.5:1 to 2:1 (partially welded) near the base of the unit and 5:1 to 10:1 (moderately to densely welded) near the top of the unit.

Pumices are generally smaller (commonly < 2 cm) and relatively sparse (5 to 30% of the rock) compared to those found in lower units. Horizontal pumice swarms contain lapilli from 5 to 14 cm in length locally. These pumice swarms suggest that unit 2 is made up of several ignimbrite deposits.

Devitrification and vapor-phase crystallization destroyed most of the original vitroclastic textures in these tuffs. Relict shards with axiolitic textures occur in a cryptocrystalline to microcrystalline groundmass. Pumices were particularly susceptible to vapor-phase alteration and typically have a granophyric texture in thin section. Hand specimens of pumice appear sugary in texture because of the deposition of coarse (up to 0.3-mm) crystals of tridymite and sanidine. Vapor-phase alteration also has resulted in both the deposition of thin mantles of alkali feldspar around sanidine phenocrysts and the oxidation of ferromagnesian phenocrysts.

The phenocryst assemblages are similar to those in units 1g and 1v, but the phenocryst abundances (17 to 20%) are slightly greater—in part as a result of the lower porosities of these more compacted tuffs (Table II, Fig. 2). Hornblende-bearing pumices similar to those described for unit 1g occur in small amounts (<5%) throughout the unit. Lithic clasts are rare (<1%) and mostly consist of devitrified rhyolitic volcanic rocks. Most lithics are <3 cm in diameter.

Well-developed fractures are characteristic of this unit. Most fractures are nearly vertical and trend N-S to N70W. Some horizontal and low-angle fractures are also present. Fracture spacing is commonly 0.2 to 2 m in the upper more densely welded portion of the tuff. Fracture apertures range from 1 mm to 4 cm. Many fractures have at least two generations of fracture-filling material. Calcite is the oldest material deposited and it commonly forms a lining up to 0.5 mm thick on the fracture walls. The centers of fractures are filled with brown clays and detritus washed into the fractures from the surface. Additional, more detailed information about fractures in unit 2 is given in the section by Wohletz (Sec. III, this report).

Nonwelded Tuff. Nonwelded tuff underlies the broad, gently sloping bench developed on top of unit 2. These nonwelded tuffs form white, soft outcrops that weather into low, rounded mounds. Talus from the overlying cliffs of unit 3 commonly covers outcrops of the nonwelded tuffs. The contact with unit 3 is gradational and is arbitrarily defined as the break in slope at the base of the uppermost cliff at TA-21. The thickness of the nonwelded unit varies from 10 m in the western part of TA-21 to 5 m in the east.

The nonwelded tuff is a pumice-poor, vapor-phase-altered ignimbrite. It consists dominantly of a white-to-light-gray, ashy matrix of shards, pumice fragments, and abundant phenocrysts. Relict shards have axiolitic textures and the groundmass is cryptocrystalline to microcrystalline. Pumice clasts are sparse (~5%) and have a sugary texture. The light-gray pumice clasts are difficult to distinguish from the light-colored tuff matrix. Pumice clasts are generally equant and range from 1 to 3 cm; rare, isolated pumices are up to 14 cm in length. Vapor-phase alteration of

these tuffs is extensive and has resulted in deposition of tridymite and sanidine in pumices, feathery overgrowths of alkali feldspar around sanidine phenocrysts, and oxidation of most ferromagnesian phenocrysts.

The phenocryst assemblage in the nonwelded unit is similar to that described for the lower units of the Tshirege Member (Table II, Fig. 2). Hornblende-bearing pumices also occur in these tuffs. One notable characteristic of these deposits is that phenocrysts are unusually abundant (21%), given the nonwelded, porous nature of these tuffs. When phenocryst abundances are corrected for porosity effects, the nonwelded unit (~35% phenocrysts) is significantly more crystal-rich than unit 2. At present, it is uncertain whether the nonwelded unit represents the nonwelded top of unit 2 or the base of unit 3. The upward increase in phenocryst contents and the abrupt change from welded tuff to nonwelded tuff suggest that the contact between the nonwelded unit and unit 2 is a partial cooling break that marks a brief hiatus in ash flow eruptions. If this is correct, the nonwelded unit is the lower part of a cooling unit that includes unit 3.

Lithic clasts are rare (<1%) and consist of light-gray, crystal-poor rhyolite and dark-gray porphyritic dacite. These clasts are typically subangular and equant. Most lithics are <4 cm in diameter.

Fractures propagate through this unit despite its nonwelded and poorly indurated nature. Calcite is the oldest fracture-filling material and commonly is deposited on fracture surfaces. The centers of fractures are commonly filled by a mixture of calcite and surface-derived detritus. Fracture apertures range from 2 to 4 cm.

Tshirege Unit 3. Unit 3 is the 16- to 18-m-thick bedrock unit that hosts the subsurface SWMUs at TA-21. Although less steep than unit 2, unit 3 is the prominent cliff-forming unit that forms the caprock of DP Mesa (see Fig. 3 of Goff, Sec. II, this report). Surface exposures are weathered to tan or orangish-tan, but fresh tuff surfaces are light gray.

Unit 3 is a nonwelded to partially welded, vapor-phase-altered ignimbrite. The tuff contains 10 to 20% crystal-rich pumice lapilli in an ashy matrix made up of shards, pumice fragments, and abundant phenocrysts. Local pumice swarms occur in the tuff and contain up to 30% pumice lapilli. Compaction of pyroclasts in the unit is slight and decreases noticeably eastward from STRAT3 to STRAT1. The matrix is white to light gray in the nonwelded tuffs and light gray with a pinkish cast in the partially welded tuffs. The preservation of relict pumices is generally good. Pumices commonly are 1 to 4 cm long and, rarely, up to 10 cm long. They are typically gray to brown and have a sugary appearance. Granophyric intergrowths of sanidine and tridymite and overlapping microcrystalline sheaves of spherulites replace the interiors of pumices. Shards are generally axiolitic and occur in a phenocryst-rich, cryptocrystalline-to-microcrystalline groundmass. Sanidine phenocrysts commonly have feathery overgrowths of alkali feldspar deposited by high-temperature vapors following emplacement of the tuffs. Ferromagnesian phenocrysts show variable degrees of oxidation resulting from vapor-phase alteration.

Phenocrysts make up 18 to 20% of these porous tuffs. Estimates of porosity-free phenocryst abundances range from 35 to 40%, reflecting an overall increase in phenocrysts from unit 1g to unit 3. Sanidine and quartz make up most of the phenocrysts, but the ratio of sanidine to quartz is greater than in underlying units (Table II, Fig. 2). The maximum size of phenocrysts is 2 to 3.5 mm. Clinopyroxene and hornblende are the dominant ferromagnesian minerals; fayalite is absent in these tuffs. Magnetite, zircon, perrierite/chevkinite/allanite, and sphene are accessory minerals. The sphene is present as

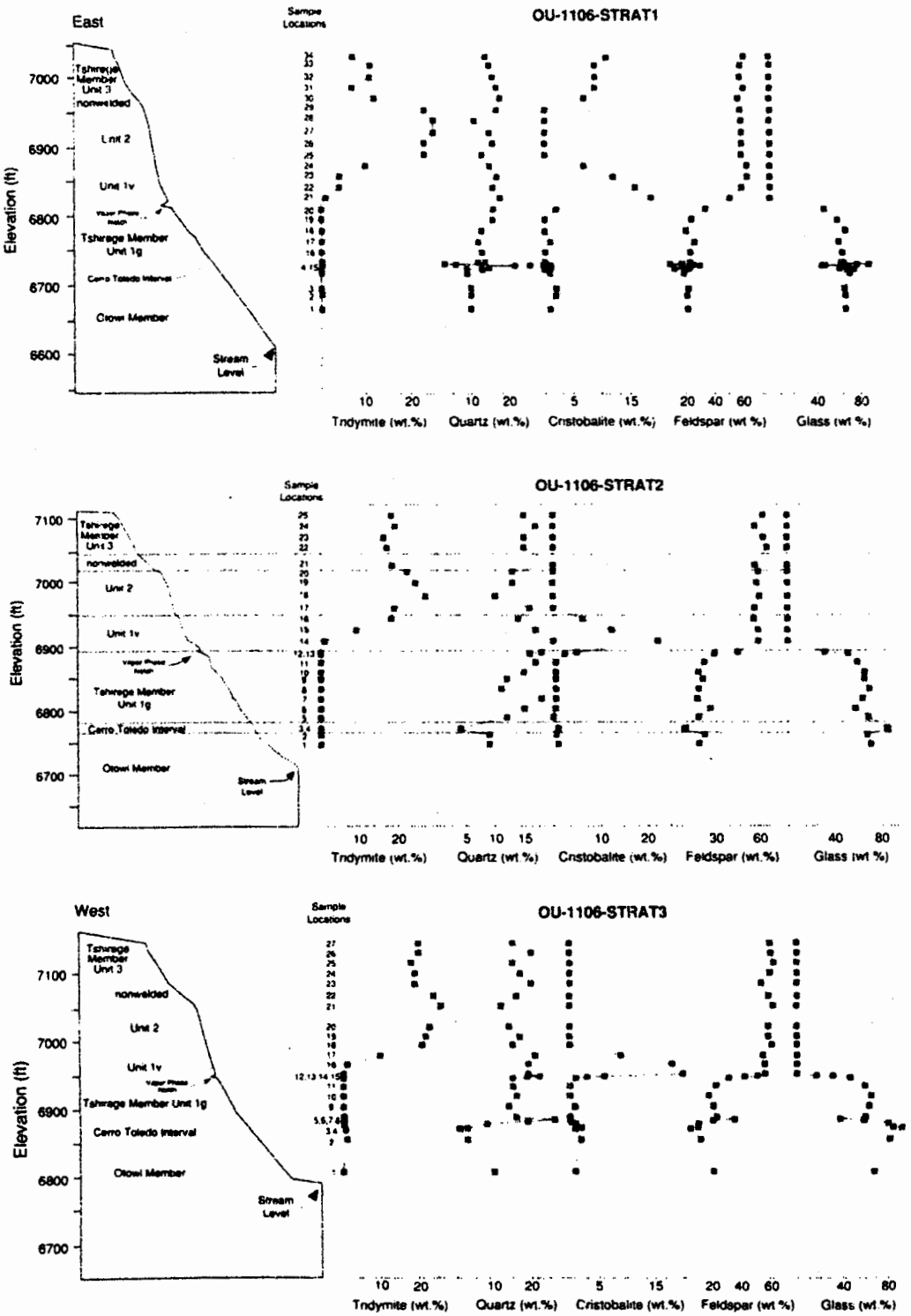

Fig. 5. Variation diagrams showing the mineralogy of tuffs in stratigraphic sections at TA-21. Canyon wall profile from FIMAD topographic base; 3x vertical exaggeration. Vapor-phase notch is also exaggerated.

TABLE IV

X-Ray Diffraction analyses of Tuffs at TA-21 [a]

Stratigraphic Section #1 (Easternmost Section)

Sample Field Number	Elevation (ft)	Unit [b]	Smectite	Tridymite	Quartz	Cristo-balite	Feldspar	Glass	Hornblende	Mica	Hematite	Magnetite	Kaolinite	Gypsum	Calcite	Σ Crystalline Phases
OU-1106-STRAT1-34	7036.2	Qbt-3	--	7 ± 1	14 ± 1	11 ± 1	62 ± 9	--	--	--	1 ± 1	--	--	--	--	95 ± 9
OU-1106-STRAT1-33	7023.4	Qbt-3	--	11 ± 1	15 ± 1	9 ± 4	60 ± 8	--	--	Tr	2 ± 1	--	--	--	--	97 ± 9
OU-1106-STRAT1-32	7006.4	Qbt-3	--	11 ± 1	16 ± 1	9 ± 4	59 ± 8	--	--	--	1 ± 1	--	--	--	--	96 ± 9
OU-1106-STRAT1-31	6990.1	Qbt-3	--	7 ± 1	17 ± 1	9 ± 4	62 ± 9	--	--	--	1 ± 1	--	--	--	--	96 ± 10
OU-1106-STRAT1-30	6974.2	Qbt-nw	--	12 ± 1	18 ± 1	7 ± 3	58 ± 8	--	--	--	1 ± 1	--	--	--	--	96 ± 9
OU-1106-STRAT1-29	6957.5	Qbt-2	--	23 ± 2	17 ± 1	--	59 ± 8	--	--	--	1 ± 1	--	--	--	--	100 ± 8
OU-1106-STRAT1-28	6941.3	Qbt-2	--	25 ± 2	11 ± 1	--	60 ± 8	--	--	--	Tr	--	--	--	--	96 ± 8
OU-1106-STRAT1-27	6924.1	Qbt-2	Tr	25 ± 2	15 ± 1	--	60 ± 8	--	--	--	1 ± 1	--	--	--	--	101 ± 8
OU-1106-STRAT1-26	6908.5	Qbt-1v	1 ± 1	23 ± 2	16 ± 1	--	60 ± 8	--	--	--	1 ± 1	--	--	--	2 ± 1	103 ± 8
OU-1106-STRAT1-25	6891.5	Qbt-1v	--	23 ± 2	13 ± 1	--	60 ± 8	--	Tr	--	1 ± 1	--	--	--	--	97 ± 8
OU-1106-STRAT1-24	6875.5	Qbt-1v	--	10 ± 1	15 ± 1	7 ± 3	64 ± 9	--	1 ± 1	Tr	2 ± 1	--	--	--	--	99 ± 10
OU-1106-STRAT1-23	6858.8	Qbt-1v	Tr	4 ± 1	17 ± 1	12 ± 1	64 ± 9	--	Tr	--	1 ± 1	--	--	--	--	98 ± 9
OU-1106-STRAT1-22	6843.3	Qbt-1v	Tr	4 ± 1	16 ± 1	16 ± 1	60 ± 8	--	Tr	--	Tr	--	--	--	--	96 ± 8
OU-1106-STRAT1-21	6827.1	Qbt-1v	--	1 ± 1	18 ± 1	19 ± 1	52 ± 7	--	Tr	--	Tr	--	--	--	--	90 ± 7
OU-1106-STRAT1-20	6810.4	Qbt-1g	--	--	16 ± 1	2 ± 1	34 ± 5	48 ± 5	Tr	--	Tr	--	--	--	--	52 ± 5
OU-1106-STRAT1-19	6794.9	Qbt-1g	Tr	--	16 ± 1	Tr	24 ± 3	60 ± 3	--	--	Tr	--	--	--	--	40 ± 3
OU-1106-STRAT1-18	6779.2	Qbt-1g	--	--	13 ± 1	Tr	20 ± 3	67 ± 3	--	--	--	--	--	--	--	33 ± 3
OU-1106-STRAT1-17	6763.2	Qbt-1g	--	--	12 ± 1	1 ± 1	26 ± 4	61 ± 4	--	--	--	--	--	--	--	39 ± 4
OU-1106-STRAT1-16	6747.4	Qbt-1g	--	--	13 ± 1	--	23 ± 3	64 ± 3	--	--	--	--	--	--	--	36 ± 3
OU-1106-STRAT1-15	6732.3	Qbt-1g	--	--	12 ± 1	--	23 ± 3	65 ± 3	--	--	--	--	--	--	--	35 ± 3
OU-1106-STRAT1-14	6731.3	Qbt-1g	--	--	14 ± 1	--	23 ± 3	63 ± 3	--	--	--	--	--	--	--	37 ± 3
OU-1106-STRAT1-13	6729.5	Qbt-1g	--	--	3 ± 1	--	9 ± 1	88 ± 1	--	--	--	--	--	--	--	12 ± 1
OU-1106-STRAT1-12	6729.2	Qbt-1g	--	--	6 ± 1	--	17 ± 2	77 ± 2	--	--	--	--	--	--	--	23 ± 2
OU-1106-STRAT1-11	6727.5	Qbt-1g	Tr	--	26 ± 2	--	25 ± 4	49 ± 4	Tr	Tr	--	--	--	--	--	51 ± 4
OU-1106-STRAT1-10	6727.3	Qct	1 ± 1	--	22 ± 2	1 ± 1	30 ± 4	46 ± 4	--	Tr	--	--	Tr	--	--	54 ± 5
OU-1106-STRAT1-9	6726.4	Qct	Tr	--	13 ± 1	--	17 ± 2	70 ± 2	--	--	--	--	--	Tr?	--	30 ± 2
OU-1106-STRAT1-8	6726.1	Qct	Tr	--	13 ± 1	Tr	24 ± 3	63 ± 3	--	--	--	--	Tr	--	--	37 ± 3
OU-1106-STRAT1-7	6723.7	Qct	Tr	--	15 ± 1	Tr	23 ± 3	62 ± 3	--	--	--	--	--	--	--	38 ± 3
OU-1106-STRAT1-6	6722.3	Qct	Tr	--	13 ± 1	--	12 ± 2	75 ± 2	--	--	--	--	--	--	--	25 ± 2
OU-1106-STRAT1-5	6722	Qbo	Tr	--	9 ± 1	1 ± 1	21 ± 3	69 ± 3	--	--	Tr	--	--	--	--	31 ± 3
OU-1106-STRAT1-4	6715.8	Qbo		--	9 ± 1	1 ± 1	19 ± 3	71 ± 3	--	--	Tr	--	--	--	--	29 ± 3
OU-1106-STRAT1-3	6692.7	Qbo	Tr	--	10 ± 1	2 ± 1	22 ± 3	66 ± 3	--	--	--	--	--	--	--	34 ± 3
OU-1106-STRAT1-2	6683.4	Qbo	Tr	--	10 ± 1	2 ± 1	21 ± 3	67 ± 3	Tr	--	--	--	--	--	--	33 ± 3
OU-1106-STRAT1-1	6662.9	Qbo	1 ± 1	--	10 ± 1	1 ± 1	21 ± 3	67 ± 3	--	--	--	--	--	--	--	33 ± 3

[a] *Mineral abundances reported as weight percent; uncertainties are two standard deviation estimates of analytical precision; -- indicates mineral not detected; Tr = trace abundance (<0.5 wt. %).*

[b] *Stratigraphic Unit - Qbo = Otowi Member of the Bandelier Tuff; Qct = Cerro Toledo interval; Qbt-1g = Tshirege unit 1g; Qbt-1v = Tshirege unit 1v; Qbt-2 = Tshirege unit 2; Qbt-nw = nonwelded tuff; Qbt-3 = Tshirege unit 3.*

TABLE IV (CONT)

X-RAY DIFFRACTION ANALYSES OF TUFFS AT TA-21

Stratigraphic Section #? (Central DP Mesa)

Sample Field Number	Elevation (ft)	Unit b	Smectite	Tridymite	Quartz	Cristobalite	Feldspar	Glass	Hornblende	Mica	Hematite	Magnetite	Kaolinite	Gypsum	Calcite	Σ Crystalline Phases
OU-1106-STRAT2-25	7103.8	Qbt-3	Tr	18 ± 1	15 ± 1	--	64 ± 9	--	--	--	1 ± 1	--	--	--	--	98 ± 9
OU-1106-STRAT2-24	7086.7	Qbt-3	Tr	19 ± 1	17 ± 1	--	58 ± 8	--	--	--	1 ± 1	-	--	--	--	95 ± 8
OU-1106-STRAT2-23	7069.3	Qbt-3	--	16 ± 1	15 ± 1	--	63 ± 9	--	--	-	1 ± 1	--	--	--	-	95 ± 9
OU-1106-STRAT2-22	7053.8	Qbt 3	--	17 ± 1	15 ± 1	--	66 ± 9	--	Tr	--	1 ± 1	--	--	--	-	99 ± 9
OU-1106-STRAT2-21	7025.9	Qbt-nw	Tr	18 ± 1	20 ± 2	--	58 ± 8	--	Tr	--	1 ± 1	--	-	--	-	97 ± 8
OU-1106-STRAT2-20	7015.8	Qbt-2	--	22 ± 2	13 ± 1	--	60 ± 8	--	--	--	1 ± 1	--	--	--	-	96 ± 8
OU-1106-STRAT2-19	6998	Qbt-2	Tr	24 ± 2	13 ± 1	--	59 ± 8	--	--	--	1 ± 1	--	Tr		--	97 ± 8
OU-1106-STRAT2-18	6977.1	Qbt-2	--	27 ± 2	10 ± 1	--	61 ± 9	--	--	--	Tr	--	-	-		98 ± 9
OU-1106-STRAT2-17	6958.2	Qbt 2	--	19 ± 1	16 ± 1	--	58 ± 8	--	Tr	--	1 ± 1	--	-	--	Tr	94 ± 8
OU-1106-STRAT2-16	6941.2	Qbt-1v		18 ± 1	14 ± 1	5 ± 2	57 ± 8	--	Tr	Tr	1 ± 1	--		-	-	95 ± 8
OU-1106-STRAT2-15	6923.7	Qbt-1v	--	9 ± 1	17 ± 1	10 ± 1	60 ± 8	--	Tr	Tr	-	-	-	-	-	96 ± 8
OU-1106-STRAT2-14	6906.6	Qbt-1v	Tr	1 ± 1	20 ± 2	18 ± 1	60 ± 8	--	--	Tr	-					99 ± 8
OU-1106-STRAT2-13	6889	Qbt-1v	--	--	18 ± 1	4 ± 1	46 ± 6	32 ± 6	Tr	-	Tr			--	--	68 ± 6
OU-1106-STRAT2-12 (pumice)	6886.5	Qbt-1g	Tr		7 ± 1	1 ± 1	20 ± 3	71 ± 3	-	--	1 ± 1			--	-	29 ± 3
OU-1106-STRAT2-12 (matrix)	6886.5	Qbt-1g	Tr	--	16 ± 1	2 ± 1	30 ± 4	52 ± 4	--	-	Tr	-		--	-	48 ± 4
OU-1106-STRAT2-11	6873.5	Qbt-1g	--	--	17 ± 1	Tr	23 ± 3	60 ± 3	Tr	--	Tr	--			-	40 ± 3
OU-1106-STRAT2-10	6858.1	Qbt-1g	--	--	15 ± 1	Tr	19 ± 3	66 ± 3	Tr	--	Tr	-		--	--	34 ± 3
OU-1106-STRAT2-9 (pumice)	6847.4	Qbt-1g	--	--	13 ± 1	Tr	12 ± 2	75 ± 2	--	--	Tr					25 ± 2
OU-1106-STRAT2-9 (matrix)	6847.4	Qbt-1g	--	--	12 ± 1	Tr	22 ± 3	66 ± 3	--	--	Tr		--	--	--	34 ± 3
OU-1106-STRAT2-8	6831.8	Qbt-1g	-	-	11 ± 1	Tr	19 ± 3	70 ± 3	--	-	--	-	-	-		30 ± 3
OU-1106-STRAT2-7	6816.6	Qbt-1g	Tr	--	18 ± 1	Tr	18 ± 3	64 ± 3	-	--	-	--	-	-	-	36 ± 3
OU-1106-STRAT2-6	6800.9	Qbt 1g	-	--	15 ± 1	Tr	27 ± 4	58 ± 4	Tr	-	Tr	-	--		--	42 ± 4
OU-1106-STRAT2-5	6788	Qbt-1g	Tr	--	12 ± 1	--	19 ± 3	69 ± 3	Tr	--	-		-		-	31 ± 3
OU-1106-STRAT2-4	6771.2	Qct	Tr	-	4 ± 1	1 ± 1	10 ± 1	85 ± 1	-	-	--	--	--			15 ± 2
OU-1106-STRAT2-3	6769.7	Qct	Tr	-	4 ± 1	1 ± 1	9 ± 1	86 ± 1	-	--	--	--		--	-	14 ± 2
OU-1106-STRAT2-2	6761.3	Qbo	Tr	--	9 ± 1	Tr	23 ± 3	68 ± 3	--	--	-			--		32 ± 3
OU-1106-STRAT2-1	6746.4	Qbo	Tr	--	9 ± 1	1 ± 1	19 ± 3	71 ± 3	-	--	-	--	-		--	29 ± 1

TABLE IV (CONT)

X-RAY DIFFRACTION ANALYSES OF TUFFS AT TA-21

Stratigraphic Section #3 (Westernmost Section)

Sample Field Number	Elevation (ft)	Unit [b]	Smectite	Tridymite	Quartz	Cristo-balite	Feldspar	Glass	Hornblende	Mica	Hematite	Magnetite	Kaolinite	Gypsum	Calcite	Σ Crystalline Phases
OU-1106-STRAT3-27	7150.8	Qbt-3		20 ± 2	15 ± 1	--	61 ± 9	--	--		1 ± 1	--				97 ± 9
OU-1106-STRAT3-26	7133.9	Qbt-3	-	20 ± 2	20 ± 2	-	62 ± 9	-	-	-	1 ± 1					103 ± 9
OU-1106-STRAT3-25	7117.7	Qbt-3	--	18 ± 1	15 ± 1	--	64 ± 9	--		--	1 ± 1					98 ± 9
OU-1106-STRAT3-24	7100.8	Qbt-3	-	19 ± 1	17 ± 1	--	61 ± 9	--	Tr	--	1 ± 1					96 ± 9
OU-1106-STRAT3-23	7084.5	Qbt-mv	--	19 ± 1	20 ± 2	-	55 ± 8		-	--	1 ± 1					95 ± 8
OU-1106-STRAT3-22	7063.7	Qbt-mv	--	24 ± 2	16 ± 1	--	60 ± 8	-	-	-			--			100 ± 8
OU-1106-STRAT3-21	7048.2	Qbt-2	--	26 ± 2	12 ± 1	--	63 ± 9	--	-	-	Tr	--				101 ± 9
OU-1106-STRAT3-20	7014.6	Qbt-2	Tr	23 ± 2	14 ± 1	--	60 ± 8	-			1 ± 1	-				98 ± 8
OU-1106-STRAT3-19	6999.0	Qbt-2	-	22 ± 2	17 ± 1	--	60 ± 8					-				99 ± 8
OU-1106-STRAT3-18	6985.8	Qbt-1v	1 ± 1	21 ± 2	15 ± 1		62 ± 9	-				-				95 ± 9
OU-1106-STRAT3-17	6968.8	Qbt-1v	-	10 ± 1	21 ± 2	9 ± 3	56 ± 8		--	--	-					96 ± 9
OU-1106-STRAT3-16	6954.3	Qbt-1v		1 ± 1	19 ± 1	18 ± 1	57 ± 8		Tr	Tr						95 ± 8
OU-1106-STRAT3-15	6937.9	Qbt-1v			19 ± 1	20 ± 2	57 ± 8	--		-	Tr	--		-		96 ± 8
OU-1106-STRAT3-14	6934.3	Qbt-1v			22 ± 2	6 ± 2	52 ± 7	17 ± 2		-	Tr	--	3 ± 1	-		83 ± 8
OU-1106-STRAT3-13	6933.2	Qbt-1g			19 ± 1	3 ± 1	43 ± 6	32 ± 6		-	Tr	-	3 ± 1	-		68 ± 6
OU-1106-STRAT3-12	6931.1	Qbt-1g			15 ± 1	1 ± 1	32 ± 4	47 ± 4			Tr	-	5 ± 1	-		53 ± 4
OU-1106-STRAT3-11	6917.5	Qbt-1g			15 ± 1	Tr	23 ± 3	60 ± 3	1 ± 1	-	Tr		1 ± 1			40 ± 3
OU-1106-STRAT3-10	6901.5	Qbt-1g	-		16 ± 1	Tr	18 ± 3	66 ± 3			Tr			Tr		34 ± 3
OU-1106-STRAT3-9	6885.0	Qbt-1g		-	14 ± 1	1 ± 1	21 ± 3	64 ± 3	-		-					36 ± 3
OU-1106-STRAT3-8	6867.7	Qbt-1g			16 ± 1		23 ± 3	61 ± 3			-	-				39 ± 3
OU-1106-STRAT3-7	6864.2	Qbt-1g			26 ± 2	-	36 ± 5	?	Tr	Tr		-				62 ± 5
OU-1106-STRAT3-6	6861.4	Qct	-		19 ± 1	--	21 ± 3	60 ± 3	-					Tr		40 ± 3
OU-1106-STRAT3-5	6857.3	Qct	-		8 ± 1	1 ± 1	10 ± 1	81 ± 1	--	-		--				19 ± 2
OU-1106-STRAT3-4	6850.7	Qct	Tr	Tr	3 ± 1	2 ± 1	10 ± 1	85 ± 1		-	-			-		15 ± 2
OU-1106-STRAT3-3	6849.5	Qct		Tr	1 ± 1	1 ± 1	5 ± 1	93 ± 1			--				-	7 ± 2
OU-1106-STRAT3-2	6831.9	Qct		1 ± 1	3 ± 1	2 ± 1	12 ± 2	82 ± 2	Tr							18 ± 3
OU-1106-STRAT3-1	6779.1	Qbo	-		10 ± 1	1 ± 1	21 ± 3	68 ± 3								32 ± 3

tiny (<0.05-mm), wedge-shaped grains in the shardy matrix. Hornblende-bearing pumices also occur in this unit.

Lithic clasts generally make up <1 to 5% of the tuff. Lithics include gray, brown, and black phenocryst-poor devitrified rhyolite, porphyritic dacite, and crystal-rich, moderately to densely welded Otowi Member. Most lithics are 1 to 7 cm in diameter, but a few are as much as 15 cm across. Despite excellent exposures in the stratigraphic sections and other cliff outcrops, there were no occurrences of the boulder deposits that were encountered near the base of unit 3 during construction of the vertical waste shafts at MDA T (Purtymun, 1969).

Mineralogy

Figure 5 shows bulk-tuff mineralogical variations at TA-21 as a function of stratigraphic position. The Bandelier and Cerro Toledo tuffs consist primarily of feldspar + quartz ± cristobalite ± tridymite ± glass (Table IV). Minor constituents include smectite, hornblende, mica, magnetite/maghemite, hematite, calcite, and kaolinite.

Volcanic glass is the major constituent (commonly >60%) of tuffs in the lower half of the stratigraphic section, including the Otowi Member, tuffs of the Cerro Toledo interval, and unit 1g of the Tshirege Member (Table IV and Fig. 5). Glass occurs as pumices and in the shardy matrix. Quartz and feldspar (sanidine) are the two other major constituents of the glassy tuffs; these crystalline phases occur as phenocrysts and as relatively minor devitrification products in the fine ash. The volcanic glass is fresh in thin section, and the absence of significant alteration minerals such as clays and zeolites strongly suggests that these tuffs have had limited contact with groundwater since their deposition. Glass abundances are fairly consistent in the upper Otowi Member and in unit 1g of the Tshirege Member. In the Cerro Toledo interval, the proportion of glass to crystalline phases varies widely because individual depositional units contain varying amounts of glassy pyroclasts, phenocrysts, and devitrified lava detritus (Fig. 5).

Volcanic glass disappears abruptly at the top of unit 1g at the vapor-phase notch (Tables III and IV; Figs. 4 and 5). Glass abundances begin to decline within 5 m of the vapor-phase notch, but most of the glass disappears within 2 m of the notch. It should be noted that, despite extensive colloquial use, the term *vapor-phase notch* is probably a misnomer because the mineral assemblage (feldspar + quartz + minor cristobalite) and textural features (lack of vapor-phase minerals lining pumices and vugs) suggest that glass underwent high-temperature devitrification without significant vapor-phase crystallization at this stratigraphic level.

Unit 1v of the Tshirege Member consists primarily of feldspar + quartz + cristobalite + tridymite. Cristobalite abundances are greatest in the colonnade tuff near the base of the unit and systematically decrease upsection (Fig. 5). Tridymite abundances vary inversely with those of cristobalite. Cristobalite is intergrown with alkali feldspar—mainly as axiolitic and spherulitic growths—and these intergrowths replace the original glassy pyroclasts that make up the tuff. These relations suggest that crystallization of colonnade tuff was largely a result of *in situ* devitrification. Tridymite, on the other hand, commonly occurs with alkali feldspar as discrete crystals and crystal aggregates that were deposited on surfaces of open pores in the tuff. Mostly likely, these occurrences of tridymite and alkali feldspar were deposited by gases rising through the tuff. The distribution of tridymite indicates that vapor-phase alteration increases systematically upsection.

Unit 2 of the Tshirege Member consists of a simple mineral assemblage of feldspar + quartz + tridymite. Tridymite is most abundant (~25%) in the moderately to densely welded tuffs of this unit (Fig. 5). Laths of

tridy
spar
tuff
coar
text
sani
degr
spor
cont
tridy
tridy

Fig. 6.
exsolu
90% o
are en
for mi
disser
for mi
light i

tridymite and equant crystals of alkali feldspar line voids in relict pumices and in the tuff matrix. The cores of some pumices are coarsely crystalline and have granophyric textures resulting from intergrowths of sanidine and quartz. Despite its greater degree of welding (and presumably a correspondingly lower permeability), unit 2 contains the highest concentrations of tridymite found in the Tshirege Member. High tridymite concentrations suggest that vapor-phase alteration was more intense in unit 2 than in other parts of the Tshirege Member. The high degree of welding and high tridymite concentrations suggest that ash flows of unit 2 were unusually hot and welded so fast that large amounts of gas was entrapped.

The nonwelded unit and unit 3 of the Tshirege Member have similar mineralogical characteristics. They both contain the assemblage feldspar + quartz + tridymite ± cristobalite.

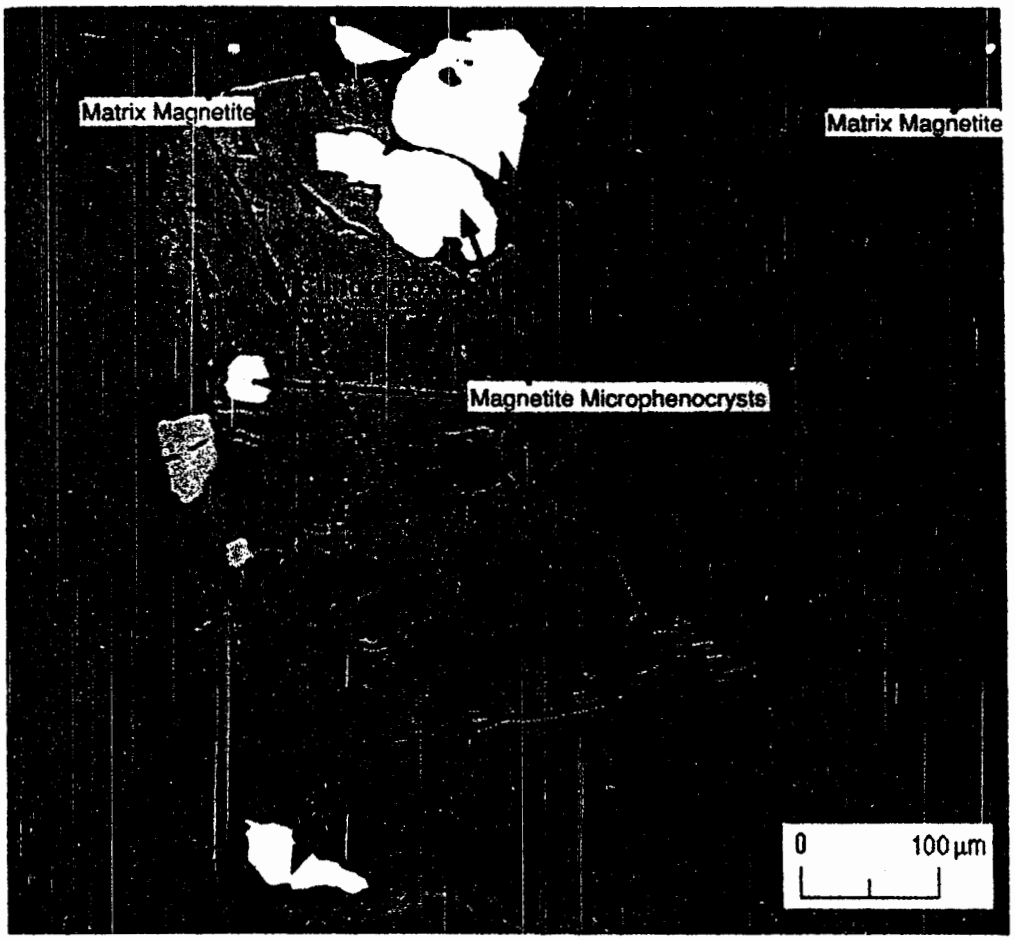

Fig. 6. Photomicrograph of magnetite microphenocrysts enclosed within a clinopyroxene phenocryst. Ilmenite exsolution lamella are visible in the lowermost magnetite grain. Magnetite microphenocrysts make up 60 to 90% of the magnetite in these tuffs. As shown in this photograph, the magnetite microphenocrysts commonly are enclosed within mafic phenocrysts; this limits their availability for mineral/water interaction. More important for mineral/water interaction are the small-matrix magnetite/hematite grains. These matrix magnetites are disseminated throughout the permeable tuff matrix and make up ~95% of the magnetite surface area available for mineral/water interaction. The sample shown here is OU-1106-STRAT3-21 from Tshirege unit 2; it is a reflected-light image.

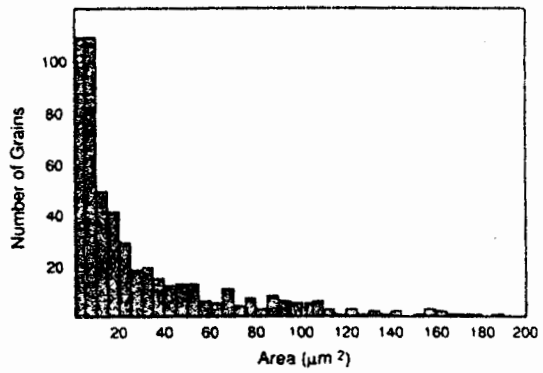

Fig. 7. Histogram of magnetite grain areas in sample 1106-STRAT2-16. Most of the grains have cross sectional areas <75 μm², and they are disseminated in the tuff matix; the remainder of magnetite grains are the relatively large microphenocrysts. Although matrix magnetites represent only 10 to 40% of the magnetite present in the rock, they provide as much as 95% of the surface area available for magnetite/water interactions. These image analysis data were collected from a thin section using reflected light (200x).

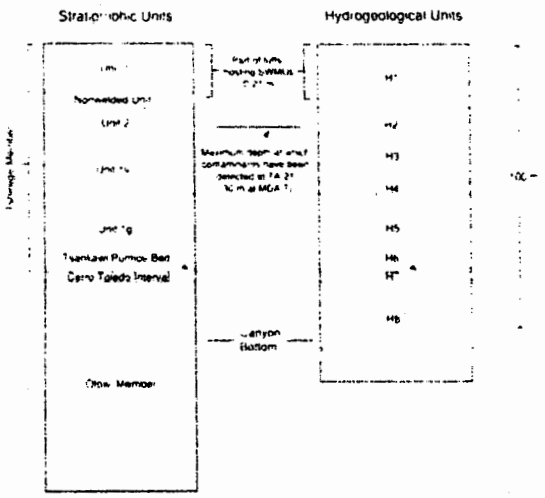

Fig. 8. Relation between stratigraphic units and preliminary proposed hydrogeological units at TA-21. The hydrogeological units generally correspond to the stratigraphic units, except for H1 and H3, which cross stratigraphic boundaries.

Though tridymite is present, its concentrations are notably less than those found in unit 2, suggesting somewhat less intense vapor-phase alteration. Cristobalite is absent in the west and central stratigraphic sections, but it is present in the east section (Table IV and Fig. 5). Tridymite abundance decreases from west to east in these units (Fig. 5). These relations suggest that vapor-phase alteration decreases eastward in the more distal portions of these tuffs.

Smectite and hematite occur in small (<2%) amounts throughout the stratigraphic sequence at TA-21 (Table IV). These two trace minerals are important because they are sorptive of certain radionuclides and could provide important natural barriers to their migration. Smectites are highly selective for cationic radionuclides (Grim, 1968). Magnetite and its alteration products, such as hematite, have an affinity for uranium and actinide species through surface-complexation (Allard and Beall, 1979; Beall and Allard, 1981; Allard *et al.*, 1982; Hsi and Langmuir, 1985; Ho and Miller, 1986). Although these minerals occur in small quantities, they are disseminated throughout the stratigraphic sequence, and their aggregate abundance and surface area available for adsorption are large when integrated over long groundwater flow paths through the tuffs.

Magnetite is present as a microphenocryst in all of the tuffs at TA-21. Its abundance commonly ranges from 0.03 to 0.2%. Magnetite grains are generally unaltered in the vitric tuffs, but some contain exsolution lamellae of ilmenite or its alteration products along 111 crystallographic directions. The magnetite shows no oxidation to maghemite in unit 1g, but varying degrees of oxidation occur in units 2 and 3. Partial to complete replacement of magnetite by hematite also occurs in the crystallized tuffs of the Tshirege Member. Former ilmenite lamellae consist of an aggregate of rutile ± hematite ± anatase (?) ± goethite. Relatively large (>75 μm² in cross section area) microphenocrysts make up only ~15% of the individual magnetite (and hematite pseudomorph) crystals observed in thin

sections (Fig. 6). Yet these few microphenocrysts account for an estimated 60 to 90% of magnetite present. The remainder of the magnetite grains are small (<75 μm^2) and occur as disseminated crystals or aggregates of crystals that are distributed uniformly throughout the matrix (Figs. 6 and 7). These smaller crystals are more important than the relatively large microphenocrysts for radionuclide retardation because they occur in the highly permeable tuff matrix and because their surface areas (based on estimates derived from grain perimeter data) account for ~96% of surface area available for mineral/water interaction.

Relation Between Stratigraphic Units and Hydrogeological Units

Figure 8 presents a preliminary representation of the major hydrogeological units for the upper part of the vadose zone at TA-21. Complete delineation of all hydrogeological units at TA-21 must await characterization of subsurface units and systematic measurements of hydrological properties from all rock units. Previous sections of this report subdivide stratigraphic units according to their mode of deposition and cooling histories. However, physical characteristics (such as permeability, bulk density, and moisture content) as well as chemical properties (such as mineralogy, rock chemistry, and water chemistry) control the movement of groundwater and contaminants through tuff. The hydrogeological zones represented in Fig. 8 are delineated by degree of welding, mineralogy, fracture characteristics, and juxtaposition of contrasting lithologies. Welding characteristics should generally correlate with hydrological properties, which are not yet determined. These hydrogeological units partly correspond with the stratigraphic units described above, but some cross stratigraphic boundaries (Fig. 8).

Hydrogeological unit H1 combines Tshirege unit 3 with the underlying nonwelded unit. Although unit 3 is partially welded near the top of the mesa, the transition into nonwelded tuffs below is gradual. The mineralogy of the nonwelded unit and unit 3 are similar. This hydrogeological unit hosts most of the subsurface SWMUs at TA-21 (Fig. 8)

Hydrogeological unit H2 consists of the moderately to densely welded, highly fractured tuffs of Tshirege unit 2. The contact between H1 and H2 represents an abrupt change in welding characteristics. Although the hydrologic properties of these tuffs have not yet been tested, hydrogeological unit 2 is expected to have significantly lower porosities and permeabilities than unit H1 because of its greater degree of welding. The sharp contrast in lithological properties across this boundary may divert groundwaters laterally where flow occurs in a porous media. This boundary may be especially important at MDA T and MDA U, where contaminants diverted laterally beneath these liquid waste sites could discharge to DP Canyon, which is developed on top of H2. Locally, where conditions favor rapid influx of recharge (for example, in drainages), groundwater flow may be controlled by the network of fractures in unit 2. Hydrogeological unit H2 is the lowest unit in which contaminated transport has been documented at TA-21 (Fig. 8 and Nyhan *et al.*, 1984).

Hydrogeological unit H3 consists of the white, slope-forming nonwelded tuffs of unit 1v. Although these tuffs probably consist of multiple flow units, the individual flows have similar lithological properties and they probably have similar hydrological properties. Because these tuffs are nonwelded, they are probably more permeable than overlying unit H2. The mineralogy of these tuffs in H3 is fairly uniform, except for the abundances of cristobalite and tridymite, which vary as a function of vertical stratigraphic position. Sorption behavior and sorption capacity of these tuffs should be unaffected by the increase in the ratio of tridymite to cristobalite upsection. These tuffs contain fractures but they are not as numerous as in unit H2.

Hydrogeological unit H4 consists of the colonnade tuffs at the base of unit 1v and includes the vapor-phase notch at its base. These tuffs are cliff-forming above the vapor-phase notch and may be incipiently welded. These tuffs have undergone *in situ* devitrification, but there is little evidence of the vapor-phase alteration that is so prevalent in overlying tuffs. Differences in welding and alteration characteristics may affect the pore structure of these rocks and cause them to have different hydrologic properties than those of the tuffs in H3. Moisture profiles from nearby drillholes commonly show increased moisture contents in this interval (for example, see Broxton *et al.*, Sec. VI, this report).

Hydrogeological unit H5 is equivalent to Tshirege unit 1g. This nonwelded ignimbrite is fairly uniform in its lithological properties, and it should be relatively permeable because of its open network of interconnected pores. The presence of abundant—and possibly reactive—glass in H5 contrasts with the devitrified mineral assemblage in H4. The ash-rich tuff at the base of the main ignimbrite and underlying surge deposits are better sorted and more stratified than the overlying massive ignimbrite. However, for now, these tuffs are included in H5 because it is not known if the occurrance of these features is widespread. These tuffs can be subdivided into separate hydrogeological units at a later date if further studies show that they are regionally extensive and that their hydrologic properties differ significantly from those of the remainder of H5.

Hydrogeological unit H6 is equivalent to the Tsankawi Pumice Bed. This pumice-fall deposit is extremely porous and is commonly associated with elevated water content in the unsaturated zone (for example, Broxton *et al.*, Sec. VI, this report). At TA-21, these pumice deposits overlie a soil horizon that may act as a perching layer. This is well illustrated in outcrops exposed in the large alcove just downstream of DP Spring, where seeps are perched within water-saturated Tsankawi Pumice Bed above fine-grain clay-rich soils.

Hydrogeological unit H7 lumps together all of the bedded deposits of the Cerro Toledo interval. These well-stratified deposits contain numerous thin depositional units characterized by a wide range of lithologies. Undoubtedly, these individual depositional units have differing hydrogeological properties. In addition, juxtaposition of lithologies with contrasting grain sizes across depositional boundaries can result in capillary and permeability barriers and cause the lateral diversion of groundwater flow. Nonetheless, these deposits are lumped together at present because their deposition in complex fluvial settings makes correlation of more finely subdivided units impractical.

Hydrogeological unit H8 is equivalent to the upper part of the Otowi Member. This nonwelded ignimbrite has fairly uniform lithological properties and should be fairly porous because of its nonwelded nature. So far only the uppermost part of this ignimbrite has been studied, and H8 may be extended to include more of the Otowi Member after further investigation.

CONCLUSIONS

Heterogeneous tuffs underlie the solid waste management units at TA-21. The physical properties of these tuffs vary both vertically and laterally. Vertical variations provide most of the geologic control for movement of groundwater in the vadose zone. Recognition of tuff heterogeneity is important for developing conceptual models of the site, evaluating transport pathways and processes, and bounding parameters in computer codes used to model groundwater and contaminant transport.

Tuff stratigraphy, with the bedrock geologic map, provides the geologic context for understanding the distribution of rock units and

forms the basis for describing cores and cuttings from future drillholes at TA-21. Depositional and cooling histories control the distribution of the major stratigraphic units whereas physical and chemical properties of the tuffs control the movement of groundwater.

Eight hydrogeological units are identified on a provisional basis (until further hydrologic testing is completed for these rocks). The hydrogeological units have unique lithological and mineralogical properties that probably affect their conductivity to water and gas. Some of these hydrogeological units cross stratigraphic boundaries. Systematic measurements of hydrological properties are necessary to complete the characterization of these units. Additional delineation of hydrogeological units in the subsurface will occur during the drilling program for the site.

The two critical bedrock units for evaluating subsurface contaminant transport at TA-21 are Tshirege unit 3 and the underlying nonwelded tuff unit that makes up hydrogeological unit H1, and Tshirege unit 2, which makes up hydrogeological unit H2. Hydrogeological unit H1 hosts both surface and subsurface SWMUs at TA-21, and its physical properties govern how contaminants are mobilized and transported at their source term. Our study shows that this hydrogeological unit is generally highly porous and contains no bedding features that might divert groundwater to canyon margins. Because of its high porosity and low degree of moisture saturation, hydrogeological unit H1 should provide an effective physical barrier to waste migration because of its ability to imbibe and trap water in the tuff matrix under natural recharge conditions. These tuffs also may provide a mineralogical barrier to contaminant migration in the tuff matrix because of the presence of trace amounts of magetite/hematite and smectite, which are highly sorptive of certain radionuclides. One area of concern is that the favorable barriers in unit H1 could be bypassed by transport through fractures. This is of particular concern at the liquid-waste MDAs, which received large amounts of effluent in addition to the natural recharge. Porous flow through the tuff matrix as well as fracture flow may have occurred beneath some of these MDAs. Preliminary observations about fracture mineralogy indicate that water from the surface has penetrated to at least the level of hydrogeological unit H2 under natural conditions.

Hydrogeological unit H2 is the lowest unit in which contaminants are documented at TA-21 (Nyhan *et al.*, 1984). Although testing of hydrologic properties of tuffs at TA-21 has not yet occurred, hydrogeological unit H2 is expected to have significantly lower porosities and permeabilities than unit H1 because of its greater degree of welding. The contrast in physical properties at the contact between H1 and H2 might provide a barrier to the downward movement of water. Such a barrier could act as a zone of accumulation for downward moving contaminants or it might divert contaminants laterally. The relative impermeability of the tuff matrix and abundance of fractures in unit H2 suggests that the RFI work plan's strategy to use slant drillholes for characterizing as many fractures as possible is warranted for the deeper boreholes being planned to investigate the liquid waste MDAs at TA-21.

ACKNOWLEDGEMENTS

We thank D. Mann and Carlos Montoya for preparing thin sections of these tuffs, many of which were difficult to mount and polish. J. Gardner, J. Wolff, P. Aamodt, C. Brause, K. Bitner, G. Eller, T. Glatzmaier, L. Maassen, J. Nyhan, S. Reneau, J. Smith, and E. Springer provided critical reviews of this report.

REFERENCES

Allard, B. and Beall, G. W., 1979, Sorption of Am on geologic media, J. Environ. Sci. Health A14 (6),.507-518.

Allard, B., Olofsson U., Torstenfelt, B., Kipasti, H., and Anderson, H., 1982, Sorption of actinides in well-defined oxidation states on geologic media, in Scientic Basis for Nuclear Waste Management V, Materials Research Society Symposia Proceedings, L. Lutze, ed. (Materials Research Society, Pittsburg, Pennsylvania), pp. 775-786.

Bailey, R. A., Smith, R. L., and Ross, C. S., 1969, Stratigraphic nomenclature of the volcanic rocks in the Jemez Mountains, New Mexico, US Geol. Survey Bull. 1274-P, 19 pp.

Baltz, E. H., Abrahams, J. H., Sr., and Purtymun, W. D., 1963, Preliminary report on geology and hydrology of Mortandad Canyon near Los Alamos, New Mexico, with reference to disposal of liquid low-level radioactive wastes, US Geological Survey open-file report (Albuquerque, New Mexico), 105 pp.

Beall, G. W. and Allard, B., 1981, Sorption of actinides from aqueous solutions under environmental conditions, in Proceedings of a Symposium on Adsorption from Aqueous Solutions, March 24-27, 1980, American Chemical Society Meeting, Division of Colloid and Surface Chemistry (Houston, Texas), pp. 193-212.

Bish, D. L. and Chipera, S. J., 1988, Problems and solutions in quantitative analysis of complex mixtures by x-ray powder diffraction, in Advances in X-Ray Analysis (Plenum Press, New York, 1988), Vol. 31, pp. 295-308.

Bish, D. L. and Chipera, S. J., 1989, Revised mineralogic summary of Yucca Mountain, Nevada, Los Alamos National Laboratory report LA-11497-MS.

Broxton, D. E., Eller, P. G., and Flores, D. 1995, Preliminary drilling results for boreholes LADP-3 and LADP-4, Sec. VI, this report, Los Alamos National Laboratory, New Mexico.

Chung, F. H., 1974a, Quantitative interpretation of x-ray diffraction patterns of mixtures. I. Matrix-flushing method for quantitative multicomponent analysis. J. App. Crystall. 7, 519-525.

Chung, F. H., 1974b, Quantitative interpretation of x-ray diffraction patterns of mixtures. II. Adiabatic principle of x-ray diffraction analysis of mixtures, J. App Crystall. 7, 526-531.

Crowe, B., Linn, G., Heiken, G., and Bevier, M., 1978, Stratigraphy of the Bandelier Tuff in the Pajarito Plateau, applications to waste management, Los Alamos National Laboratory report LA-7225-MS, 57 p.

Fisher, R. V. and Schmincke, H.-U., 1984, Pyroclastic Rocks (Springer-Verlag, Berlin), 472 p.

Gardner, J. N., Kolbe, T., and Chang, S., 1993, Geology, drilling, and some hydrologic aspects of Seismic Hazards Program Core Holes, Los Alamos National Laboratory, New Mexico, Los Alamos National Laboratory report LA-12460-MS, 19 p.

Goff, Fraser, 1995, Geologic Map of TA-21, Sec. VI, this report, Los Alamos National Laboratory, New Mexico.

Griggs, R. L., 1964, Geology and ground-water resources of the Los Alamos area, New Mexico, US Geological Survey water-supply paper 1753, 107 p.

Grim, R. E., 1968, Clay Mineralogy, 2nd ed. (McGraw-Hill Book Company, New York), 596 p.

Heiken, G., Goff, F., Stix, J., Tamanyu, S., Shafiqullah, S., Garcia, S., and Hagan, R, 1986, Intracaldera volcanic activity, Toledo caldera and embayment, Jemez Mountains, New Mexico, J. Geophys. Res. 91(B2), 1799-1815.

Ho, C. H. and Miller, N. H., 1986, Adsorption of uranyl species from bicarbonate solution onto hematite particles, J. Colloid Interface Sci. 110, 165-171.

Hsi, C-K and Langmuir, 1985, Adsorption of uranyl onto ferric oxyhydroxides: Application of the surface complexation site-binding model, Geochim. Cosmochim. Acta. 49, 1931-1941.

Izett, G. A. and Obradovich, J. D., 1994, $^{40}Ar/^{39}Ar$ age constraints for the Jaramillo Normal Subchron and the Matuyama-Brunhes geomagnetic boundary, J. Geophys. Res. 99(B2), 2925-2934.

Klug, H. P. and Alexander, L. E., 1974, X-Ray Diffraction Procedures for Polycrystalline and Amorphous Materials (John Wiley & Sons, Inc. New York).

Nyhan, J. W., Drennon, B. J., Abeele, W. V., Trujillo, G., Herrera, W. J., Wheeler, M. L., Booth, J. W., and Purtymun, W. D., 1984, Distribution of radionuclides and water in Bandelier Tuff beneath a former Los Alamos liquid waste disposal site after 33 years, Los Alamos National Laboratory report LA-10159-LLWM, 51 pp.

Peterson, D. W., 1979, Significance of the flattening of pumice fragments in ash-flow tuffs, Geological Society of America special paper 180, pp. 195-204.

Purtymun, W. D., 1969, Correspondence from W. E. Hale, District Chief, Water Resources Division, US Geological Survey, to C. W. Christenson, H-7 Group Leader, Subject: Geology at Disposal Area Near Bldg. 257, TA-21, April 19, 1969, 2 pp.

Reneau, S., 1995, Geomorphic studies of DP Mesa and vicinity, Sec. VI, this report, Los Alamos National Laboratory, New Mexico.

Smith, R. L., 1960a, Zones and zonal variations in welded ash flows, US Geological Survey professional paper 354-F, pp. 149-159.

Smith, R. L., 1960b, Ash flows, Geol. Soc. Am. Bull. 71, 795-842.

Smith, R. L. and Bailey, 1966, The Bandelier Tuff: a study of ash-flow eruption cycles from zoned magma chambers, Bull. Volcanol. 29, 83-104.

Smith, R. L., Bailey, R. A., and Ross, C. S., 1970, Geologic map of the Jemez Mountains, New Mexico, US Geological Survey Map I-571, scale 1:1250000.

Stoker, A. K., McLin, S. G., Purtymun, W. D., Maes, M. N., and Hammock, B. G., 1992, Water supply at Los Alamos during 1989, Los Alamos National Laboratory report LA-12276-PR, 51 p.

Vaniman, D. and Wohletz, K., 1990, Results of geological mapping/fracture studies, TA-55 area, Los Alamos National Laboratory Seismic Hazards memorandum EES1-SH90-17.

Vaniman, D. and Wohletz, K., 1991, Revisions to report EES1-SH90-17, Los Alamos National Laboratory seismic hazards memorandum EES1-SH91-12.

Weir, J. E. and Purtymun, W. D., 1962, Geology and hydrology of Technical Area 49, Frijoles Mesa, Los Alamos County, New Mexico, US Geological Survey adminstrative release report, Albuquerque, New Mexico, 225 pp.

Wohletz, K., 1995, Measurement and analysis of rock fractures in the Tshirege Member of the Bandelier Tuff along Los Canyon adjacent to TA-21, 1995, Sec. II, this report, Los Alamos National Laboratory, New Mexico.

Contents

Abstract 1

Introduction 1
D.E. Broxton and P.G. Eller

Geologic Map of Technical Area 21 7
F. Goff

Measurement and Analysis of Rock Fractures in the Tshirege Member of the Bandelier Tuff along Los Alamos Canyon Adjacent to Technical Area-21 19
K. H. Wohletz

Stratigraphy, Petrography, and Mineralogy of Bandelier Tuff and Cerro Toledo Deposits 33
D.E. Broxton, G.H. Heiken, S.J. Chipera, and F.M. Byers, Jr.

Geomorphic Studies at DP Mesa and Vicinity 65
S.L. Reneau

Preliminary Drilling Results for Boreholes LADP-3 and LADP-4 93
D.E. Broxton, P.A. Longmire, P.G. Eller, D. Flores

Fluorescein Dye Experiment at DP Spring and Sewage Outfall 111
A. Adams, J. DeMuth, D. Counce, and F. Goff

LA-12934-MS

UC-903
Issued: June 1995

Earth Science Investigations for Environmental Restoration— Los Alamos National Laboratory Technical Area 21

Edited by
D.E. Broxton
P.G. Eller

Los Alamos
NATIONAL LABORATORY
Los Alamos, New Mexico 87545